

---

# Current challenges using models to forecast seawater intrusion: lessons from the Eastern Shore of Virginia, USA

Ward E. Sanford · Jason P. Pope

**Abstract** A three-dimensional model of the aquifer system of the Eastern Shore of Virginia, USA was calibrated to reproduce historical water levels and forecast the potential for saltwater intrusion. Future scenarios were simulated with two pumping schemes to predict potential areas of saltwater intrusion. Simulations suggest that only a few wells would be threatened with detectable salinity increases before 2050. The objective was to examine whether salinity increases can be accurately forecast for individual wells with such a model, and to address what the challenges are in making such model forecasts given current (2009) simulation capabilities. The analysis suggests that even with current computer capabilities, accurate simulations of concentrations within a regional-scale (many km) transition zone are computationally prohibitive. The relative paucity of data that is typical for such regions relative to what is needed for accurate transport simulations suggests that even with an infinitely powerful computer, accurate forecasting for a single well would still be elusive. Useful approaches may include local-grid refinement near wells and geophysical surveys, but it is important to keep expectations for simulated forecasts at wells in line with chloride concentration and other data that can be obtained at that local scale.

**Keywords** Numerical modeling · Salt-water/fresh-water relations · USA

## Introduction

Given that a substantial proportion of the earth's population lives along coastlines, and that global warming may create

noticeable sea-level rises over the next century, water-resource managers face a long-term struggle in safeguarding existing coastal fresh groundwater supplies from the hazards of seawater intrusion from natural and anthropogenic causes. The characteristics of transition zones between freshwater and saltwater in coastal aquifers and the dynamics of their movements have been understood for several decades (Todd 1959; Cooper et al. 1964). With the advent of digital computers, numerical algorithms and solution methods were developed to solve the equations for variable-density groundwater flow and transport that represent saltwater intrusion (Pinder and Cooper 1970; Segol and Pinder 1976). Computer codes then became available to simulate saltwater intrusion for user-specified aquifer geometries and characteristics in the two dimensions of a cross-sectional profile (Voss 1984; Sanford and Konikow 1985). The availability of mathematical tools has promoted a growing interest in the study and forecasting of saltwater intrusion hazards (Bear et al. 1999).

Two-dimensional models are capable of tracking a saltwater transition zone as it migrates landward in reaction to groundwater extractions in the freshwater aquifer, but flow in the vicinity of a well has attributes of cylindrical symmetry parallel to the well, and thus three-dimensional flow and transport occur inevitably as landward-migrating saltwater approaches a well. Thus, in order to use a mathematical model to try to forecast the increases in salinity that might occur in a particular extraction well under such circumstances, a three-dimensional simulation is an inescapable requirement. Computer speed and storage capabilities have increased dramatically in the last few decades, to the point where three-dimensional simulations of saltwater intrusion can be accomplished with reasonable computation times with the latest simulation codes (Voss and Provost 2002; Langevin et al. 2003). One issue that continues to make three-dimensional simulations a challenge is the tendency of transition zones to be relatively narrow in the vertical dimension and the fine grid resolution required to solve the advective-dispersion equation accurately under such conditions. Although certain numerical techniques have proven to be more efficient than others in simulating narrow transition zones in two dimensions (Sanford and Konikow 1985; Voss and Souza 1987; Cox and Nishikawa 2001), simulating these zones in three dimensions is still a challenge.

Accurate forecasting of saltwater intrusion into extraction wells by the use of models requires an accurate description

---

Received: 7 January 2009 / Accepted: 1 August 2009  
Published online: 25 August 2009

© US Government 2009

---

W. E. Sanford (✉)  
US Geological Survey,  
Mail Stop 431, 12201 Sunrise Valley Dr., Reston, VA 20192, USA  
e-mail: wsanford@usgs.gov  
Tel.: +1-703-6485882  
Fax: +1-703-6485274

J. P. Pope  
US Geological Survey,  
1730 East Parham Road, Richmond, VA 23228, USA

and simulation of the transport of saltwater both on the regional scale of the transition zone and in the local vicinity of the well. Theoretically, the three-dimensional codes that are available today can simulate both scales simultaneously, but such an accurate forecasting simulation remains to be demonstrated for field conditions with the types and amount of data that are available (Post 2005).

A study is presented here of a three-dimensional saltwater intrusion model where the available data were fairly abundant, yet typical of many coastal settings. Different objectives might exist for such a saltwater intrusion model. One objective might be to simply ascertain whether or not the current transition zone is in equilibrium with respect to modern-day sea level. Another objective might be to ascertain whether or not the transition zone will encroach to the location of a given well within, say, 50 years. Either of these objectives might be feasible for a three-dimensional saltwater intrusion model because the predictions are not very specific. On the other hand, what many water managers want to know is when and by how much chloride concentrations will increase in a specific well. This latter type of specific forecasting of saltwater intrusion is what was ultimately desired by the water managers on the Eastern Shore of Virginia. The purpose of this paper is to consider the potential accuracy and results of this model and consider whether, in practice, it is possible to accurately forecast saltwater intrusion at specific wells using such a model, both from the standpoint of model construction and the availability of data. A discussion is presented whether the current limitations for making a reasonably accurate model forecast of a chloride increase at a given well is the limited computational power or limited amount of data.

## Study area

### Geographic setting

The study area is situated along the Atlantic Ocean to the east of the Chesapeake Bay in the Coastal Plain Physiographic Province (Fig. 1). Two counties, Accomack and Northampton, make up the area known as the Eastern Shore of Virginia (Fig. 2a). The Eastern Shore is a peninsula that is about 110 km long and 15-30 km wide, and covers approximately 2,000 km<sup>2</sup>. It is bounded on the east by the Atlantic Ocean, the south and west by the Chesapeake Bay, and the north by the State of Maryland. The model area extends into the State of Maryland and includes offshore areas in the Chesapeake Bay and the Atlantic Ocean. The offshore areas are included to allow the model to simulate interaction between the fresh and saline groundwaters. The Eastern Shore is dominated by a 9-13 m ridge that runs down the center of the peninsula and is covered by marshes along the coasts and a combination of agriculture and forest in the center (Fig. 2).

### Geologic setting

The sedimentary deposits that make up the Eastern Shore generally thicken and dip northeastward, and range in thickness from about 600 m west of the peninsula to about 2,000 m east of the peninsula (Meng and Harsh 1988). These sediments generally overlie a hard-rock surface, commonly referred to as the “basement,” that also dips northeastward. The lower 70% of the sediments are of Early to Late Cretaceous age and were deposited in fluvial environments (Robbins et al. 1975). The remaining 30% of the sediments are Tertiary and Quaternary in age and were deposited in mostly marine environments (Cushing et al. 1973). The Miocene deposits that are of interest in this study are the St.

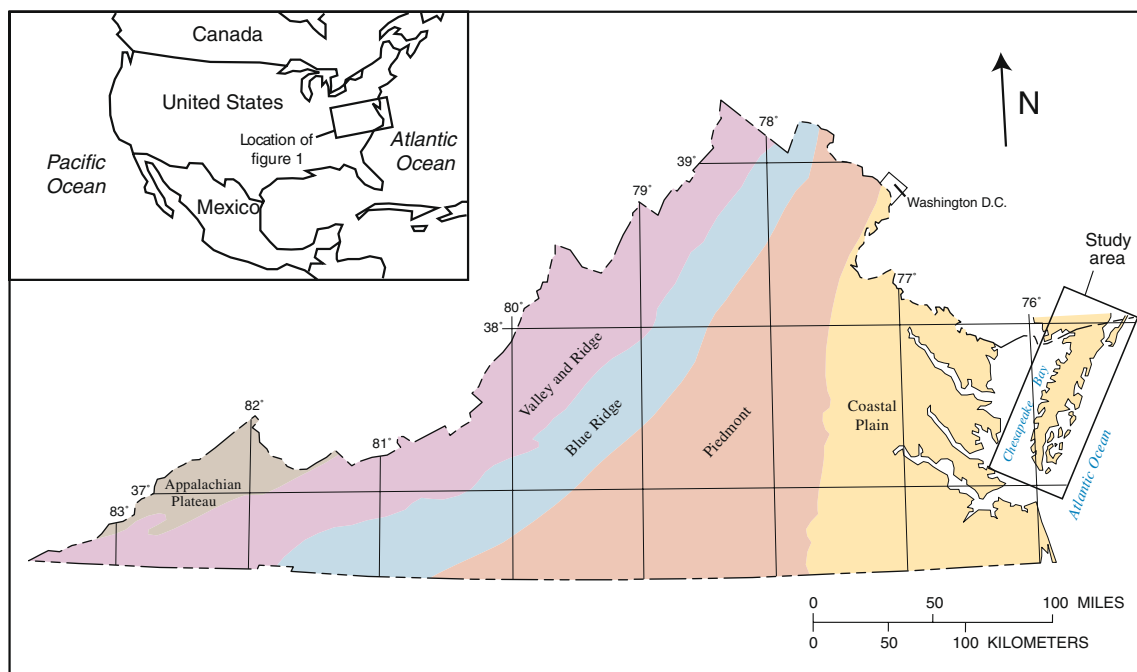


**Fig. 1** Physiographic provinces of Virginia and the location of the study area

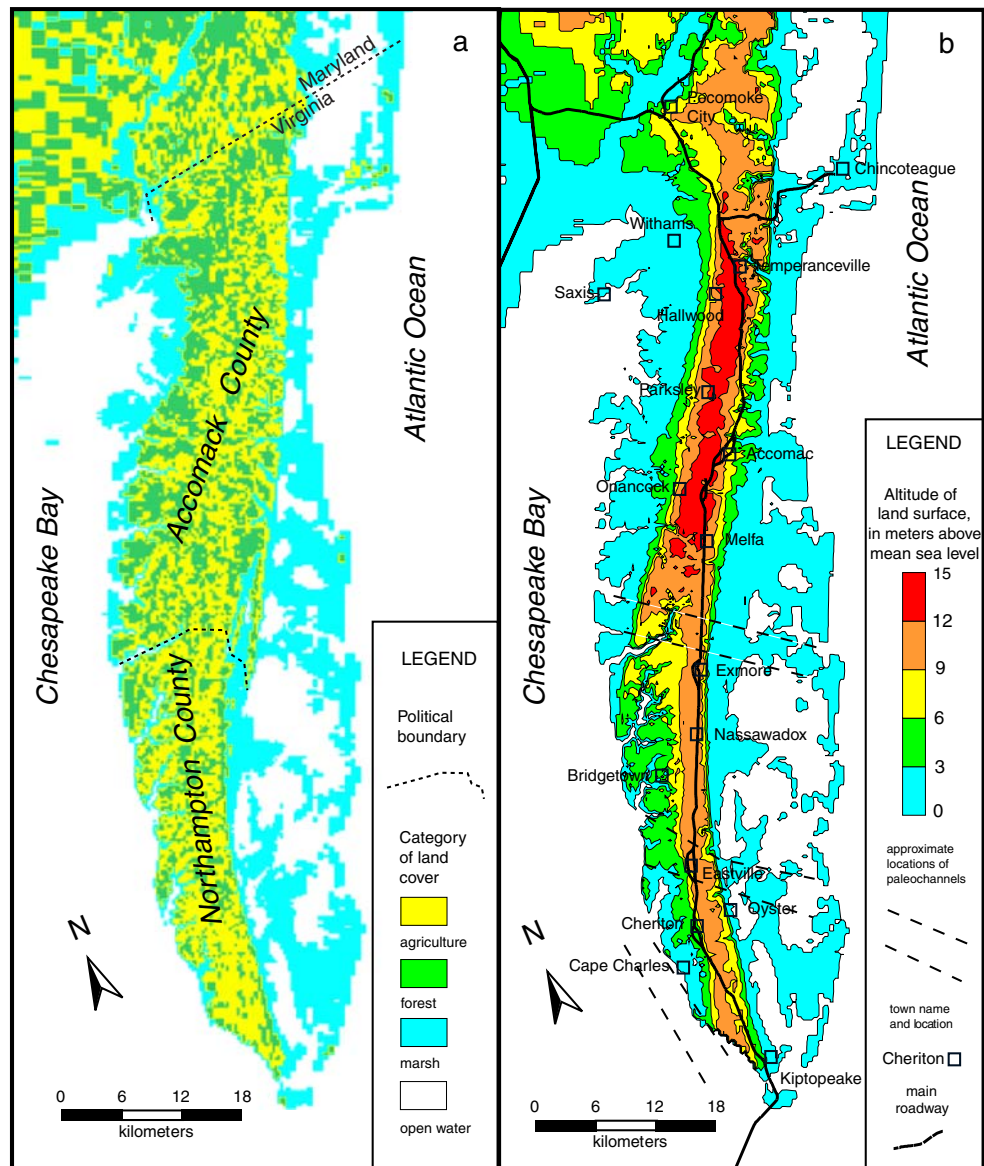


**Fig. 2** Maps showing **a** generalized land cover categories and political boundaries, and **b** land surface topography and locations of towns and paleochannels. Land surface data are from the USGS 30-m National Elevation Dataset and National Land Cover Database

Marys and Eastover Formations of the Chesapeake Group. The St. Marys Formation is a massive, mostly dense, well-sorted, clayey silt that is approximately 100 m thick. The Eastover Formation overlies the St. Marys and consists of massive to laminated, muddy, fine sand interbedded with finer and coarser-grained beds and ranges between approximately 30 and 100 m thick. The Yorktown Formation of Pliocene age consists of commonly shelly, very-fine to coarse quartz sand interbedded with sandy and silty clay to clayey silt that ranges between approximately 30 to 100 m thick. During the Pleistocene Epoch, channels were eroded across the Eastern Shore into previously deposited sediments. These channels were eroded during sea-level low stands and were filled during high stands. Three such major paleochannels are known to exist near the towns of Cape Charles, Eastville, and Exmore (Mixon 1985). The remaining sediments of Quaternary age were deposited in marginal-marine and estuarine environments, including those

of Holocene-age that make up the salt-marsh, back-bay, and barrier-island sediments around the edges of the peninsula. The sediments of Quaternary age range in thickness from approximately 10 to 40 m.

### Hydrogeologic setting

The regional hydrogeology groundwater-flow system in the Atlantic Coastal Plain has recently been studied by McFarland and Bruce (2006) and simulated by Heywood and Pope (2009). The Eastern Shore flow system is a local flow system within this regional flow system. Sediments beneath the Eastern Shore have historically been divided on the basis of hydrologic properties into a layered sequence of aquifers and confining units (Richardson 1994). The aquifers consist of predominantly sand- and gravel-size material of sufficient saturated thickness to yield substantial quantities of water. The confining units

consist of predominantly very fine sand, silt, and clay; and are generally continuous across the Eastern Shore (except where eroded by paleochannels), yield little water, and retard its movement. The hydrogeologic framework for this study includes a surficial (unconfined) aquifer, a series of three confined aquifers and confining layers, and a basal confining unit (Sanford et al. 2009a). The confined aquifer system is shallower than 100 m; its components are termed the upper, middle, and lower Yorktown-Eastover (YE) aquifers and confining units. This combined name has been the accepted nomenclature for all six hydrogeologic units because the boundary between the Eastover and overlying Yorktown Formations is not always located precisely at the boundary between one of the units, although usually the Eastover Formation coincides with the two lower YE units. The thicknesses and range of reported hydraulic conductivities of the aquifers and confining layers are listed in Table 1.

Two major paleochannels were included in the hydrogeologic framework of this study. The northern channel, near the town of Exmore (Fig. 2) and the southern channel near the town of Eastville. The maximum thicknesses of the Exmore and Eastville channels in the central Eastern Shore are approximately 30 and 20 m, respectively. The surficial aquifer is unconfined throughout the Eastern Shore and overlies the upper YE confining unit, and ranges in thickness from approximately 1 to 25 m. The surficial aquifer consists primarily of sediment from the Pleistocene formations, which lithologically varies widely in composition (Sinnott and Tibbott 1968). The water table is expressed at the surface as the small ponds and streams throughout the Eastern Shore.

### Hydrologic setting

Annual rainfall on the Eastern Shore is approximately 100 cm. Runoff on the Eastern Shore is relatively low, leading to streams that are relatively small and few in number. Given that in humid climates about two-thirds of rainfall is lost to evapotranspiration and the remaining one-third either runs off or recharges the water table, the annual recharge here is estimated to range between 30 and 40 cm. Groundwater flows mostly laterally from the recharge areas in the central upland and discharges along the coastal bays (Speiran 1996), but a small percentage will move vertically downward through the upper Yorktown-Eastover confining unit into the confined aquifer system (Fig. 3). Water in the confined aquifers eventually migrates vertically back upward across the confining layers to discharge to the coastal bays. As the groundwater approaches the coastal

bays, it comes into contact with the brackish water beneath the coastal saltwater bodies, creating a freshwater/saltwater transition zone. Natural water levels in the wells (Fig. 4a) across the Eastern Shore reflect this flow system. Water levels in the central upland area are higher than those at the coast. Also, in the central upland, water levels in the upper aquifers are higher than those in the lower aquifers. In contrast, along the coast, water levels in the lower aquifers are slightly higher than those in the upper aquifers.

In September and October of 2003, 51 wells from across the Eastern Shore at 18 sites (Fennema and Newton 1982) were sampled for groundwater chemistry (Fig. 4b). A summary of the results from this sampling is given in Table 2 and Sanford et al. (2009a). In order to determine if saltwater intrusion was occurring, chloride was measured in these wells and compared to wells that were sampled in the early 1980s (Richardson 1994). The lack of a substantial increase in average chloride concentrations between the early 1980s and 2003 suggests saltwater intrusion is not currently a widespread problem on the Eastern Shore, although there are known problems locally. Sulfur hexafluoride, SF<sub>6</sub>, was measured in wells that were completed in the surficial aquifers to provide ages against which the recharges rates to the surficial aquifer could be calibrated.

Carbon-14 was also measured in the 51 wells, but because of the abundant shell fragments in many of the formations, it was determined that carbon-14-based ages were not well enough constrained to use in the model calibration.

Detailed bathymetry and salinity distributions around the Eastern Shore are given in Sanford et al. (2009a). Depths of water in the Chesapeake Bay are relatively shallow, but a paleo-river channel exists in the southern part of the bay close to land where water depths exceed 30 m. In this section of the bay, the upper confined aquifer may have a direct connection to the saltwater in the bay. The salinity of seawater is 35 parts per thousand (ppt), and salinities in the coastal bays on the ocean side do not fall much below this as the runoff of freshwater from the land is relatively small there. In the Chesapeake Bay, the salinity values decrease from near seawater at the mouth of the Bay to about half of that of seawater at the northwest coastline of the Eastern Shore. Salinity within the bay also varies with water depth and season, but average values were used for calculations in this study.

Groundwater is the main source of freshwater on the Eastern Shore, and categories of its use include domestic, agricultural, industrial, and public supply. Before the mid-1960s, groundwater withdrawals were less than 4,000 cubic meters per day (CMD) and were predominantly for domestic and agricultural use. Beginning in the late-1960s,

**Table 1** Ranges of thickness and hydraulic conductivities reported for the confined hydrogeologic units

Hydrogeologic unit name	Range of thicknesses (m)	Hydraulic conductivity (m/s)
Upper Yorktown-Eastover Confining Unit	1–35	No data
Upper Yorktown-Eastover Aquifer	1–30	1.2E-05–2.1E-04
Middle Yorktown-Eastover Confining Unit	1–25	No data
Middle Yorktown-Eastover Aquifer	3–25	1.5E-05–1.6E-04
Lower Yorktown-Eastover Confining Unit	2–25	No data
Lower Yorktown-Eastover Aquifer	5–60	5.6E-06–8.5E-05
St. Marys Confining Unit	15–120	4.0E-11

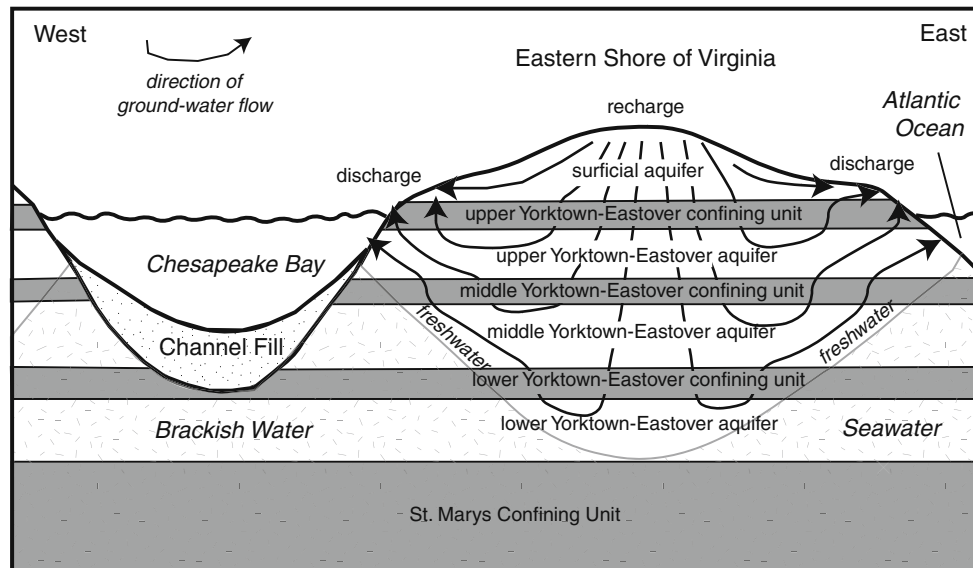


Fig. 3 Schematic diagram of groundwater flow in the Eastern Shore of Virginia

industrial and public supply withdrawals increased to about 1,200 CMD for Accomack County and 6,000 CMD for Northampton County. Since the 1970s, the withdrawals in Accomack County have increased to about 16,000 CMD, whereas the withdrawals in Northampton County are currently below 4,000 CMD, primarily because saltwater intrusion began to be a problem that forced users to curtail pumping. The proportion of water used under different categories has not changed dramatically since the 1980s. Industrial use is the largest category consistently in Accomack County, with two chicken processing plants being the largest users. Irrigation use can also be high but varies dramatically from year to year depending upon the amount of rainfall received during the growing season. The proportion of water drawn from each confined aquifer has been approximately equal, with about 30% from the lower aquifer and 35% each from the middle and upper aquifers.

### Groundwater model development

In order to better assess the impact of future withdrawals on water levels and salinity in the aquifer system, the USGS code SEAWAT2000 (Guo and Langevin 2002; Langevin et al. 2003) was used to construct a model to simulate water-level and chloride-concentration changes (Sanford et al. 2009a). The hydraulic properties of the model were varied in space until a best fit was obtained with historical water-level data given the magnitude and distribution of pumpage that has occurred on the Eastern Shore. The automated parameter estimation code UCODE (Poeter and Hill 1998) was used to facilitate finding the optimal parameter values and to evaluate the sensitivity of the parameters to the observations.

### Model grid

The model required a numerical grid with a resolution that could represent topographic variations in the horizontal

dimension and the transition zone between freshwater and saltwater in the vertical dimension. The grid contains 370 rows, 102 columns, and 46 layers for a total of 1,736,040 cells. The cells are 328 m  $\times$  328 m in the central part of the grid and up to 656 m  $\times$  1640 m in the corners of the model area. The hydrogeologic units generally follow the model layers (Fig. 5), and are comprised of between 2 and 8 model layers each. The number of model layers is greater than the number of hydrogeologic layers in order to better approximate the saltwater transition zone. The solute-transport equation was solved using standard finite differences with upstream weighting. Upstream weighting reduces numerical oscillations for simulations that have sharp concentration fronts relative to the grid spacing (Zheng and Bennett 1995). Although upstream weighting creates more numerical dispersion than the more computationally intensive alternatives, there are few field data that define the average width of the transition zone beneath the Eastern Shore, and the alternative of making the grid finer or employing a solution algorithm with less numerical dispersion was beyond the capability of current computing power.

### Boundary conditions

Boundary conditions for the model include specified flux to simulate recharge at the land surface, and head-dependent flux to simulate evapotranspiration from the water table, and leakage across the floor of the Atlantic Ocean, the Chesapeake Bay, the other coastal saltwater bodies, and the northern land boundary with Maryland. The remaining sides and bottom of the model are specified as no-flow boundaries.

Recharge was specified to the land-surface areas of the model by zone. The zones were delineated based on soil type and slope. Soils with high, moderate, and low permeabilities were mapped into the three recharge zones used in the model. Cells with a high topographic slope were shifted into a recharge zone with the next lower

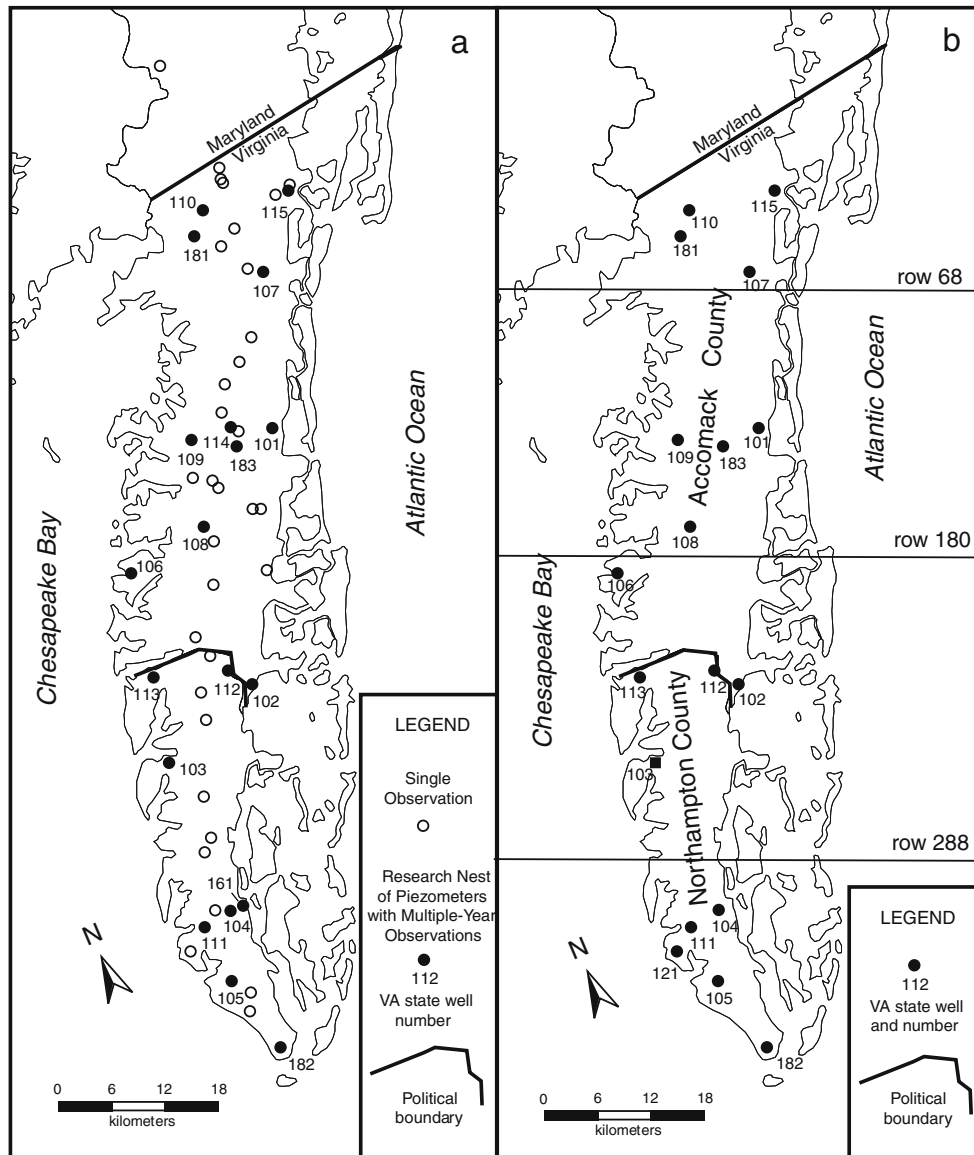


**Fig. 4** Locations of wells in the Yorktown-Eastover aquifer that were sampled for groundwater **a** levels and **b** chemistry. Individual model rows shown indicate locations of cross sections in Fig. 5

permeability class to represent the lower recharge caused by increased runoff. The magnitude of recharge assigned to these zones were estimated by an inverse simulation procedure that produced the best fit of water-level observations in the surficial aquifer and ages calculated from the sulfur hexafluoride ( $\text{SF}_6$ ) measurements (Sanford et al. 2009a). The surficial aquifer hydraulic conductivities and recharge rates were estimated separately from and before the YE parameters were estimated, as the water levels in the surficial aquifer do not respond noticeably to pumping in the confined aquifers. After the YE parameters were estimated, the surficial aquifer and recharge parameters were re-estimated, but their values changed very little. The final estimated recharge values were 60, 30, and 18 cm/year for the high, moderate, and low recharge zones, respectively.

Evapotranspiration (ET) from the water table is widespread across the Eastern Shore because of the

relatively shallow depth to the water table, especially in the low-lying coastal areas. ET is simulated in the model by assigning a maximum ET flux when the water table is at the land surface and an extinction depth below which the ET flux becomes zero. The ET flux decreases linearly with water-table altitude between the specified land surface and ET extinction depth. The extinction depth is often approximated by the average depth of the root zone, which for this study was based on the land-cover type (Fig. 2a). The extinction depths in the forest, agricultural, and marsh regions were set to 180, 90, and 60 cm, respectively. The single maximum ET rate was estimated simultaneously with the recharge rates and surficial aquifer hydraulic conductivities.

For the cells in the top layer of the model that are overlain by water, a general-head boundary condition was used to allow the conductance term to represent water covering the cell. The head for each general-head cell is

**Table 2** Observed chloride concentrations and specific conductance. See Fig. 4 for well locations

Virginia State Well number	Well name	Well depth (m)	Aquifer	Cl <sup>-</sup> mg/L in 1980s	Cl <sup>-</sup> mg/L in 2003	Spec. Cond. $\mu$ S in 2003
SOW 101A	BAYLY'S NECK	46.3	YE upper	8	9	237
SOW 101B	BAYLY'S NECK	67.1	YE middle	8	8	240
SOW 101C	BAYLY'S NECK	89.0	YE lower	88	96	605
SOW 102A	OCEANSIDE	46.9	YE upper	51	46	519
SOW 102B	OCEANSIDE	67.1	YE middle	350	377	1671
SOW 102C	OCEANSIDE	93.3	YE lower	2100	2100	7070
SOW 103A	PC KELLAM	11.3	Surficial	23	31	417
SOW 103B	PC KELLAM	40.2	YE upper	35	32	435
SOW 103C	PC KELLAM	71.6	YE middle	290	238	1136
SOW 104A	DOTTIES GROCERY	42.7	YE upper	19	21	277
SOW 104B	DOTTIES GROCERY	73.1	YE middle	14	18	249
SOW 104C	DOTTIES GROCERY	94.5	YE lower	130	128	631
SOW 104S	DOTTIES GROCERY	11.0	Surficial	32	20	228
SOW 105A	CAPE CENTER	39.6	YE upper	25	26	416
SOW 105B	CAPE CENTER	59.7	YE middle	11	13	310
SOW 105C	CAPE CENTER	86.9	YE lower	92	79	887
SOW 105S	CAPE CENTER	6.1	surficial	No data	40	243
SOW 106A	HACK'S NECK	11.3	YE upper	363	220	837
SOW 106B	HACK'S NECK	29.0	YE upper	39	197	1072
SOW 106C	HACK'S NECK	53.6	YE middle	310	393	1709
SOW 107A	CHESSIR BROTHERS	42.7	YE upper	8	9	246
SOW 107B	CHESSIR BROTHERS	62.8	YE middle	8	8	227
SOW 107C	CHESSIR BROTHERS	93.0	YE lower	14	13	333
SOW 108A	MELFA	15.2	Surficial	18	24	386
SOW 108B	MELFA	54.9	YE upper	8	8	213
SOW 108C	MELFA	86.6	YE middle	11	10	274
SOW 109B	BAYSIDE	69.5	YE lower	15	12	418
SOW 109C	BAYSIDE	88.4	YE lower	515	No data	No data
SOW 109S	BAYSIDE	7.6	surficial	19	16	247
SOW 110A	WITHAMS	39.6	YE upper	14	13	410
SOW 110B	WITHAMS	54.3	YE middle	82	63	839
SOW 110C	WITHAMS	73.1	YE lower	1150	741	3429
SOW 110S	WITHAMS	11.0	Surficial	16	14	104
SOW 111A	CHERITON	45.7	YE upper	6	6	290
SOW 111B	CHERITON	85.3	YE middle	9	7	301
SOW 111C	CHERITON	100.6	YE lower	630	625	2339
SOW 112A	WILLIS' WHARF	41.1	YE upper	12	18	403
SOW 112B	WILLIS' WHARF	64.0	YE middle	35	36	446
SOW 112C	WILLIS' WHARF	95.4	YE lower	1,700	1,550	5,830
SOW 113A	CONCORDS WHARF	36.6	YE upper	24	14	220
SOW 113B	CONCORDS WHARF	68.6	YE middle	1400	No data	No data
SOW 113C	CONCORDS WHARF	88.4	YE lower	6200	No data	No data
SOW 115E	CHINCOTEAGUE	85.3	YE middle	140	144	828
SOW 121	BROWN & ROOT	57.9	YE middle	No data	165	835
SOW 181C	JENKIN'S BRIDGE	103.6	YE lower	2100	2370	7906
SOW 181D	JENKIN'S BRIDGE	70.1	YE lower	810	270	1487
SOW 181E	JENKIN'S BRIDGE	9.1	Surficial	23	18	155
SOW 182C	KIPTOPEKE	67.1	YE lower	59	63	673
SOW 182D	KIPTOPEKE	18.3	YE upper	32	46	336
SOW 182E	KIPTOPEKE	6.1	surficial	24	46	390
SOW 183A	ACCOMAC	86.9	YE lower	No data	49	489
SOW 183B	ACCOMAC	71.6	YE middle	No data	7	248
SOW 183C	ACCOMAC	41.1	YE upper	No data	9	204
SOW 183D	ACCOMAC	6.1	surficial	No data	32	380

adjusted for density internally by SEAWAT2000 using the specified head value (zero for sea level), the altitude of the cell below sea level, and the surface-water chloride concentration at that cell.

The northern land boundary of the model is not a hydrologic boundary, and could not be represented accurately by either a no-flow or constant-head condition. In order to prevent unrealistic effects on simulated heads, a general-head boundary was assigned.

The conductance term can be adjusted along that boundary to control the simulated water levels in that region. The conductance term is set relatively low, so the northern boundary contributes negligible water to the model. Hydrologic conditions in Maryland have only a small influence on water levels in Virginia, so the northern boundary conductance term was not adjusted extensively to create a best-fit to observed water levels in Maryland.

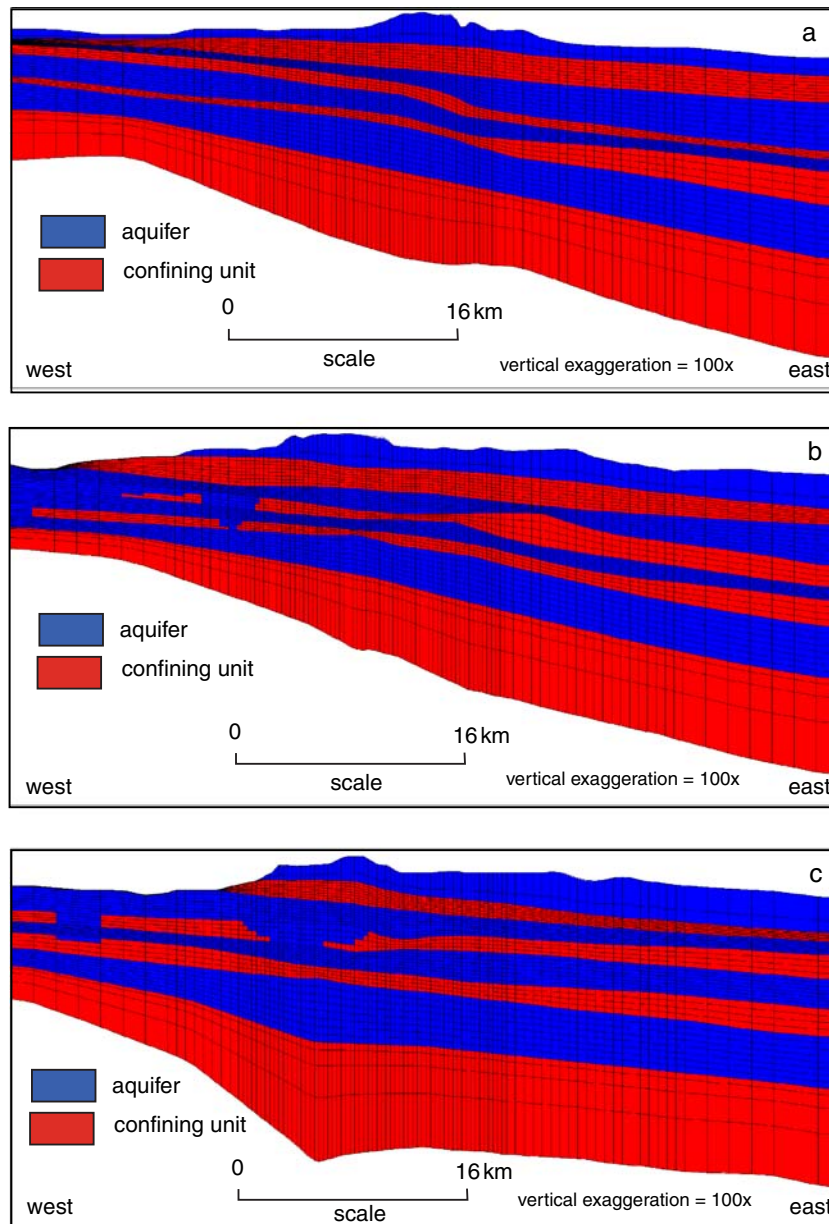


**Fig. 5** Cross-sectional views of the model grid at rows **a** 68, **b** 180, and **c** 288. The rows are numbered increasing toward the south. Breached confining layers from the paleochannels are visible in **(b)** and **(c)**. See Fig. 4b for locations of model grid rows along the peninsula

### **Historic withdrawals**

Historically most groundwater on the Eastern Shore was extracted from shallow wells in the surficial aquifer for domestic and small-business use. During the twentieth century, as drilling became more practical and affordable, more wells were drilled in the confined aquifers and fewer in the unconfined aquifer. To create a model that is reliable for assessing current pumping effects on future water levels, it was first necessary to simulate observed historical water levels and historical withdrawals. Industrial, commercial, public-supply, and some agricultural withdrawals from individual wells were assigned to the model using the multi-node-well package (Halford and Hanson 2002). Pre-1982 pumping estimates were taken from Richardson (1994).

Withdrawals from the surficial aquifer were not included in the historical simulations for several reasons. First, records of withdrawals from the surficial aquifer are sparse. Second, much of the domestic withdrawal has migrated to the confined aquifers to avoid contamination from pollution at the land surface. Third, recharge rates in the surficial aquifer are quite large compared to individual withdrawals, so water-level declines are usually limited to near the withdrawal wells, and are less likely in observation wells.

Beginning in 1982, permits were required by the Virginia Department of Environmental Quality (DEQ) for withdrawals greater than 1,200m<sup>3</sup>/month. The actual withdrawals for these wells were entered into the model. Withdrawal rates increased dramatically in the late 1960s,

**Table 3** Estimated and specified values of hydraulic parameters for the model of the Eastern Shore of Virginia. All values are estimated except for the specified values marked with the letter superscripted a (see footnote);  $K$  hydraulic conductivity,  $S_s$  specific storage. See Fig. 6 for locations

Pilot point no.	Pilot Point Name	K (m/s) Upper confining unit	K (m/s) Middle confining unit	K (m/s) Lower confining unit	Ss (1/m) All confining units	Ss (1/m) All aquifers	K (m/s) Upper aquifer	K (m/s) Middle aquifer	K (m/s) Lower aquifer	K (m/s) Surficial aquifer	Total number
1	Pocomoke	2.75E-09	1.06E-10	3.17E-08	3.30E-05 <sup>a</sup>	1.30E-05 <sup>a</sup>	6.35E-05	6.70E-05	2.65E-04 <sup>a</sup>	2.65E-04 <sup>a</sup>	
2	Withams	2.54E-09	1.31E-10	2.82E-10	3.30E-05 <sup>a</sup>	1.30E-05 <sup>a</sup>	1.76E-06 <sup>a</sup>	3.53E-06	1.76E-06 <sup>a</sup>	2.65E-04 <sup>a</sup>	
3	Jenkin's Bridge	1.27E-08	7.41E-11	7.06E-09	3.30E-05 <sup>a</sup>	1.30E-05 <sup>a</sup>	1.76E-06 <sup>a</sup>	2.65E-04 <sup>a</sup>	3.53E-06 <sup>a</sup>	2.65E-04 <sup>a</sup>	
4	Chincoteague	3.53E-09	3.53E-11	1.66E-08	5.25E-04	1.30E-05 <sup>a</sup>	8.11E-05	1.69E-05	2.65E-04 <sup>a</sup>	2.65E-04 <sup>a</sup>	
5	Tyson's	1.94E-09	2.12E-08	4.59E-10	4.92E-04	1.30E-05 <sup>a</sup>	2.54E-05	2.93E-05	4.90E-05	2.65E-04 <sup>a</sup>	
6	Temperanceville	2.12E-09	2.65E-08	7.06E-09	4.27E-04	1.30E-05 <sup>a</sup>	2.12E-05	2.12E-04	5.29E-06	2.65E-04 <sup>a</sup>	
7	Bayside	2.33E-09	2.29E-09	3.17E-10	3.30E-05 <sup>a</sup>	1.30E-05 <sup>a</sup>	1.76E-06 <sup>a</sup>	2.65E-04 <sup>a</sup>	3.67E-05	1.76E-04 <sup>a</sup>	
8	Perdue	2.96E-09	3.53E-09	1.83E-09	3.30E-05 <sup>a</sup>	1.30E-05 <sup>a</sup>	8.11E-06	1.76E-06 <sup>a</sup>	2.61E-05	1.76E-04 <sup>a</sup>	
9	Accomac	3.53E-09	9.17E-09	1.87E-10	3.30E-05 <sup>a</sup>	1.30E-05 <sup>a</sup>	9.88E-05	6.70E-05	2.54E-05	1.76E-04	
10	Bayly's Neck	5.15E-09	2.22E-09	2.50E-09	3.30E-05 <sup>a</sup>	1.30E-05 <sup>a</sup>	1.83E-04	1.09E-05	1.73E-05	1.76E-04	
11	Melfa	7.06E-09	2.47E-09	3.17E-10	3.30E-05 <sup>a</sup>	1.30E-05 <sup>a</sup>	3.53E-06 <sup>a</sup>	3.53E-06 <sup>a</sup>	3.53E-06 <sup>a</sup>	1.76E-04 <sup>a</sup>	
12	Hack's Neck	1.34E-10	1.80E-07 <sup>a</sup>	1.80E-07 <sup>a</sup>	3.30E-05 <sup>a</sup>	1.30E-05 <sup>a</sup>	2.65E-04 <sup>a</sup>	1.13E-04	1.06E-05	1.76E-04 <sup>a</sup>	
13	Concord's Wharf	1.41E-10	1.80E-07 <sup>a</sup>	1.80E-07 <sup>a</sup>	3.30E-05 <sup>a</sup>	1.30E-05 <sup>a</sup>	2.65E-04 <sup>a</sup>	1.06E-04	1.06E-05	8.82E-05 <sup>a</sup>	
14	Exmore	1.83E-10	1.80E-07 <sup>a</sup>	1.06E-08	1.64E-04	1.30E-05 <sup>a</sup>	3.53E-06 <sup>a</sup>	2.65E-04 <sup>a</sup>	2.65E-04 <sup>a</sup>	8.82E-05 <sup>a</sup>	
15	Oceanside	3.10E-10	7.06E-08	9.17E-08	3.30E-05 <sup>a</sup>	1.30E-05 <sup>a</sup>	2.65E-04 <sup>a</sup>	2.65E-04 <sup>a</sup>	2.65E-04 <sup>a</sup>	8.82E-05 <sup>a</sup>	
16	Bridgetown	2.19E-09	2.65E-09	2.47E-10	6.56E-05	1.30E-05 <sup>a</sup>	1.76E-06 <sup>a</sup>	1.76E-06 <sup>a</sup>	2.65E-04 <sup>a</sup>	8.82E-05 <sup>a</sup>	
17	Cape Charles	1.20E-09	1.76E-08	1.80E-07 <sup>a</sup>	1.00E-03	1.30E-05 <sup>a</sup>	2.65E-04 <sup>a</sup>	1.76E-06 <sup>a</sup>	2.47E-05	3.53E-04 <sup>a</sup>	
18	Cheriton	1.87E-09	1.16E-08	1.80E-07 <sup>a</sup>	1.00E-03	1.30E-05 <sup>a</sup>	1.76E-06 <sup>a</sup>	1.76E-06 <sup>a</sup>	1.76E-06 <sup>a</sup>	3.53E-04 <sup>a</sup>	
19	Oyster	1.62E-08	2.15E-09	1.09E-10	2.79E-04	1.30E-05 <sup>a</sup>	3.53E-06 <sup>a</sup>	3.53E-06 <sup>a</sup>	1.76E-06 <sup>a</sup>	3.53E-04 <sup>a</sup>	
20	Stingray's	4.59E-10	1.41E-08	1.20E-11	1.00E-03 <sup>a</sup>	1.30E-05 <sup>a</sup>	1.76E-06 <sup>a</sup>	1.76E-06 <sup>a</sup>	2.82E-06	3.53E-04 <sup>a</sup>	
21	Kiptopeake	3.46E-09	1.80E-07 <sup>a</sup>	5.64E-08	1.00E-03 <sup>a</sup>	1.30E-05 <sup>a</sup>	2.65E-04 <sup>a</sup>	1.76E-06 <sup>a</sup>	1.76E-06 <sup>a</sup>	3.53E-04 <sup>a</sup>	
	Median value	2.33E-09	9.17E-09	7.06E-09	3.01E-04	1.30E-05 <sup>a</sup>	2.12E-05	1.69E-05	1.73E-05	2.65E-04	
	Mean value	3.47E-09	4.25E-08	4.44E-08	3.01E-04	1.30E-05 <sup>a</sup>	8.69E-05	8.10E-05	7.36E-05	2.27E-04	
	Number estimated	21	17	17	6	0	7	9	10	4	91
	Number specified	0	4	4	15	21	14	12	11	17	81

<sup>a</sup> Specified values

and the rates have been approximately evenly distributed between the three confined aquifers, with a total withdrawal rate for the Eastern Shore of about 5,000 CMD in 2003. Accomack County withdrawals have exceeded those of Northampton County by a factor of about 3–4. The Maryland counties within the model area have had withdrawal rates similar to or less than that of Northampton County.

Domestic withdrawals are not reported, so instead they were estimated based on the temporal and spatial distribution of the population on the Eastern Shore. The following algorithm, also used for the entire Virginia Coastal Plain in another study (Pope et al. 2007), was used to determine the magnitude and distribution of domestic pumpage. First, each individual is assumed to use 0.3 CMD. The population was mapped based on census-block groups from the 2000 census. People within a census-block group are assumed to live along roads. Areas serviced by public-supply wells were excluded. Coverages representing public-supply areas, roads, and population were combined in a Geographic Information System (GIS) to assign flow rates to model grid cells. This allowed the withdrawals to be distributed where people are likely to be living, rather than uniformly across the entire Eastern Shore. It was assumed that domestic wells were completed in the deeper aquifers in greater numbers starting in the 1940s, and that by the 1960s, most domestic wells were in the confined aquifers. Thus domestic pumping does not begin in the model until 1940, and it increases linearly until 1960 when it reaches the rate for the entire self-supplied population. The pumping is distributed between the upper, middle, and lower aquifers based on the distribution of well screens from a sampling of well installation records from Accomack and Northampton counties (Pope et al. 2007).

### Hydraulic parameters

The automated inverse model calibration tool UCODE was used to adjust hydraulic parameter values until a best fit was obtained between the observed and simulated water levels. The calibration data included 189 observation wells that have water-level observations over many years; many of the observation wells are part of 18 nests of wells shown in Fig. 4, and are completed in the four different aquifers at the individual sites. Depending upon their sensitivity, parameters representing hydraulic conductivity and specific storage for the confined system were either estimated or assigned values (Table 3). As mentioned earlier, the surficial aquifer, recharge and maximum ET parameters were estimated first, followed by the parameters for the confined system. Porosities were assigned best-estimated values. Some parameter values could not be constrained by the calibration procedure, because the simulated observations were relatively insensitive to the parameter values. Values for these insensitive parameters were specified within the reasonable range of values that might be expected in the study area. Data from hydraulic tests such as pumping or specific capacity tests were not used directly. Although values from such tests were used to estimate reasonable values and limits for the parameters, they typically sample only a few hundred meters or less of the

formation nearest the test site, and were therefore not assigned as values in this regional-scale model.

For this study, it was decided that values between hydrogeologic units would vary discretely, but that spatially the values within the units would vary gradually. Within each unit, the hydraulic conductivity was assumed to be isotropic both in the vertical and horizontal directions. To vary the values gradually in space, a technique was used that combined pilot points with kriging. In this model, 21 pilot-point locations were selected (Fig. 6). Although different strategies have been employed for locating pilot points (Doherty 2002), the points in this study were made coincident with observation-well nest locations. The degree to which the value of each pilot point influences the values in the areas surrounding the point was calculated, and is represented by contours of percentage influence (Fig. 6). The kriged fields of parameter values (hydraulic conductivity and specific storage)

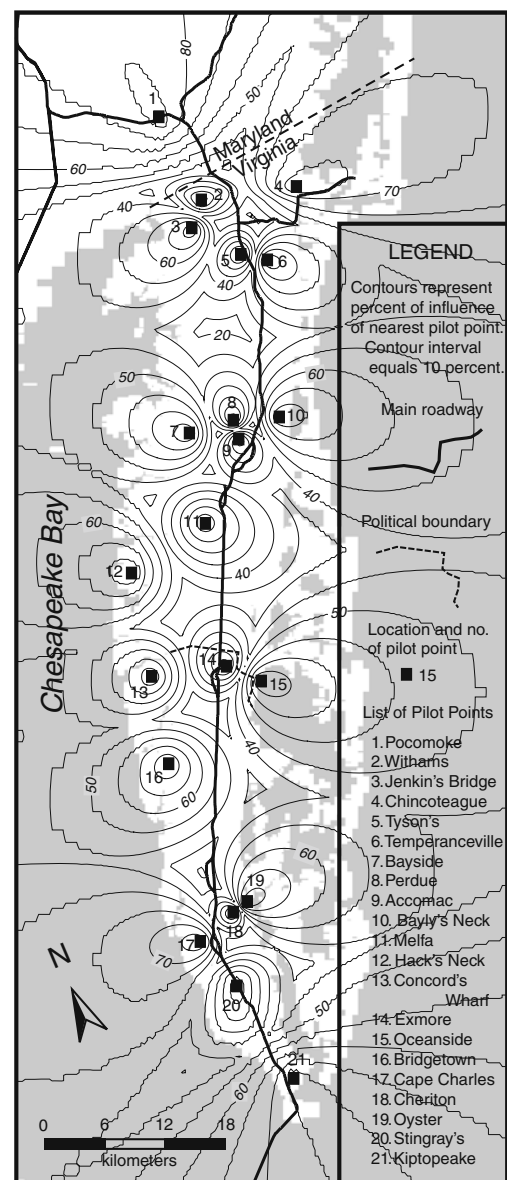


Fig. 6 Areas of influence for each of the parameter pilot points used for model calibration

were calculated based on the logarithms of the actual parameter values (Sanford et al. 2009a)

In the spring of 2006, cores were obtained in Northampton County from the entire vertical thickness of the flow system. Based on data from these cores (Sanford et al. 2009b), the aquifers were assigned a porosity value of 40% and the confining units a value of 50%. These values are of total, not effective, porosity. These two values may be close in regional systems with slow groundwater movement, as effective and total porosity can become indistinguishable at low velocities in homogeneous material (Neretnieks 1981). A value close to total porosity is used in this study, as saltwater encroachment is a long-term, slow process on a regional scale.

It was discovered during the calibration procedure that the water levels were very insensitive to the specific storage of the aquifer, and only sensitive to specific storage of confining units near substantial pumping. Consequently, all values of the specific storage for all of

the aquifers were assigned a value of  $1.3 \times 10^{-5} \text{ m}^{-1}$ . The values for the confining units were assigned upper and lower bounds of  $1 \times 10^{-3}$  and  $3 \times 10^{-5} \text{ m}^{-1}$ , respectively, beyond which the values were not adjusted to improve fit. These values are typical of the specific-storage values for sediment types in these units (Domenico and Mifflin 1965).

Hydraulic conductivity values for the confined aquifers were estimated at the pilot-point locations by the calibration procedure. Observations and historical pumping histories allowed for the estimation of many values in Accomack and the northernmost part of Northampton County, but values could not be reliably estimated for much of southern Northampton County. The values of hydraulic conductivity were given upper and lower bounds of  $2.7 \times 10^{-4}$  and  $1.8 \times 10^{-6} \text{ m/s}$ , respectively. The calibrated hydraulic conductivity and transmissivity fields of the lower and upper Yorktown-Eastover aquifers are shown in Figs. 7 and 8, respectively. The simulated locations of the paleochannels are

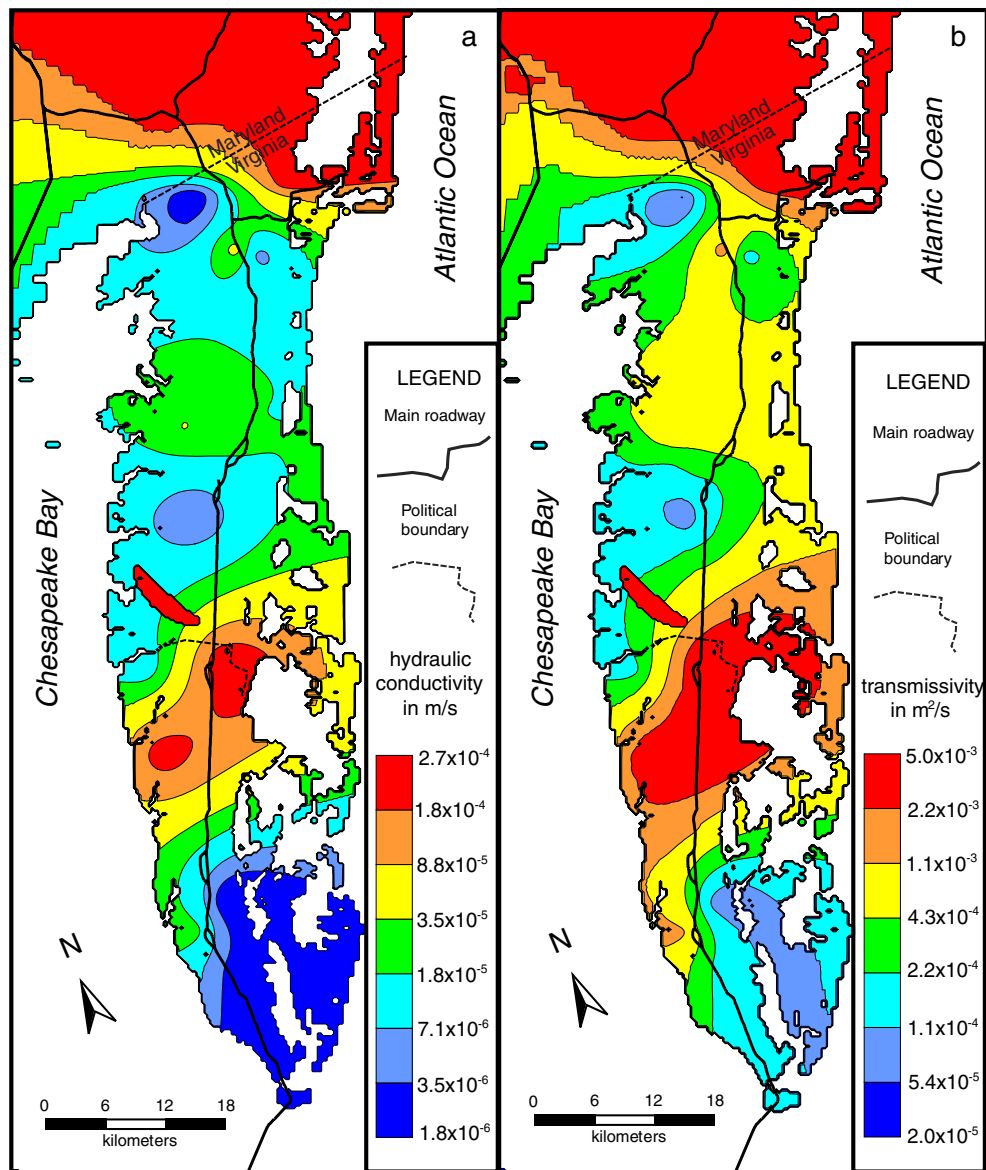


Fig. 7 The calibrated a hydraulic conductivity, and b transmissivity of the lower Yorktown-Eastover aquifer

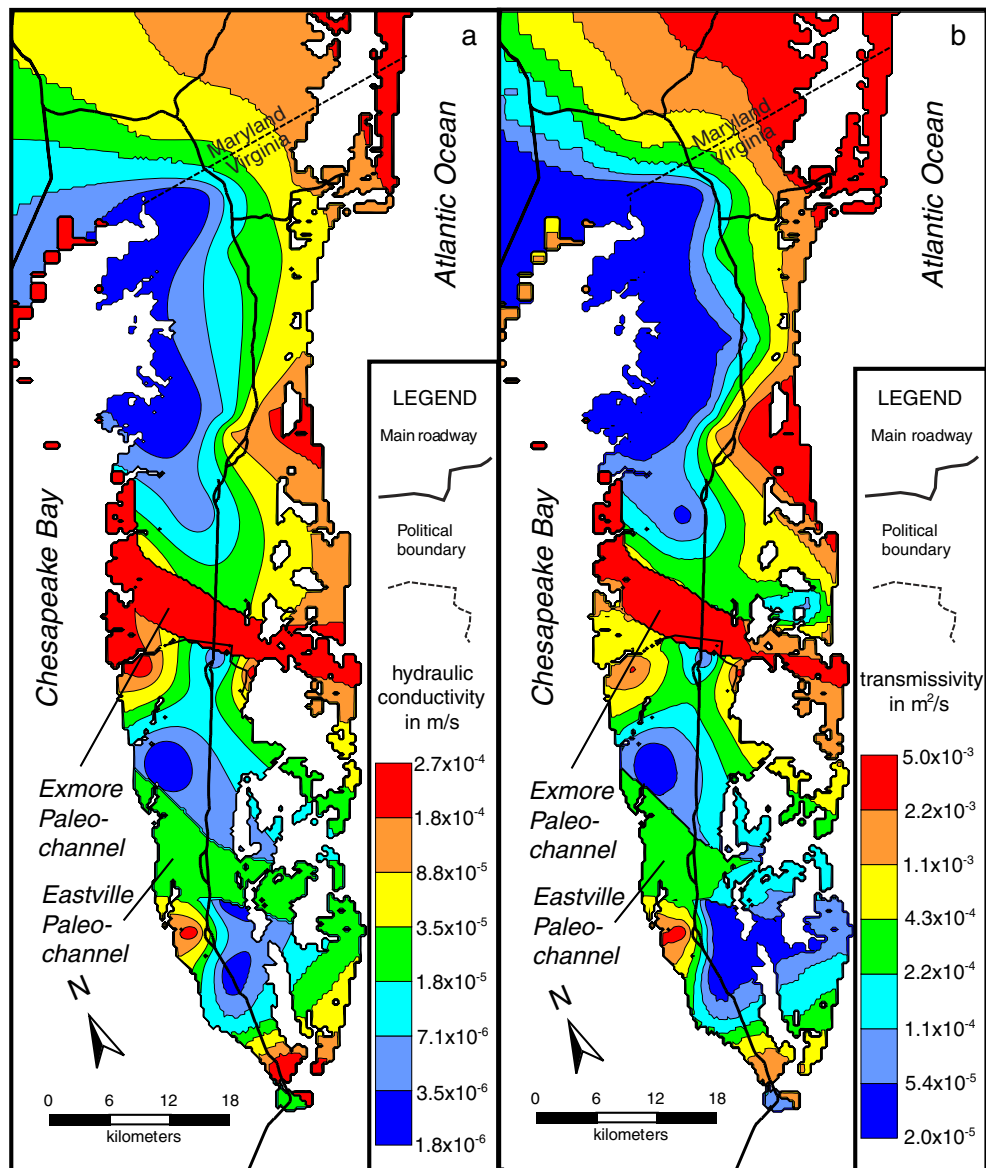


Fig. 8 The calibrated a hydraulic conductivity, and b transmissivity of the upper Yorktown-Eastover aquifer

discernable in Fig. 8 because they were assigned hydraulic conductivity values distinct from the aquifer and confining units that they transect. As a whole, the simulated water levels were more sensitive to the hydraulic conductivity values of the confining units than of the aquifers. This is because the pre-development water levels are controlled more by the confining units than by the aquifers. The calibrated hydraulic conductivity and vertical leakance fields of the upper Yorktown-Eastover confining unit are shown in Fig. 9. Additional details of the calibrated parameters and their sensitivities and confidence intervals can be found in Sanford et al. (2009a).

### Groundwater model simulations

Model-calibration simulations had a start time at the beginning of 1900 and an end time at the end of 2003. Each

year was considered to be a separate stress period in SEAWAT, and each stress period was divided into four time steps. The model was calibrated by running flow simulations with an approximate representation of the saltwater transition zone. Transient transport was simulated after the hydraulic parameters had been estimated, during which the pre-development chloride-concentration field was adjusted to fit the known conditions beneath the Eastern Shore. Further calibration following the adjustment of the chloride-concentration field did not create any substantial changes in the estimates of the parameter values.

### Simulated water levels

Simulated water levels for predevelopment conditions (the year 1900) are shown in Fig. 10. Overall, the highest water levels are beneath the central-upland ridge. Water levels in the surficial aquifer resemble the land-surface

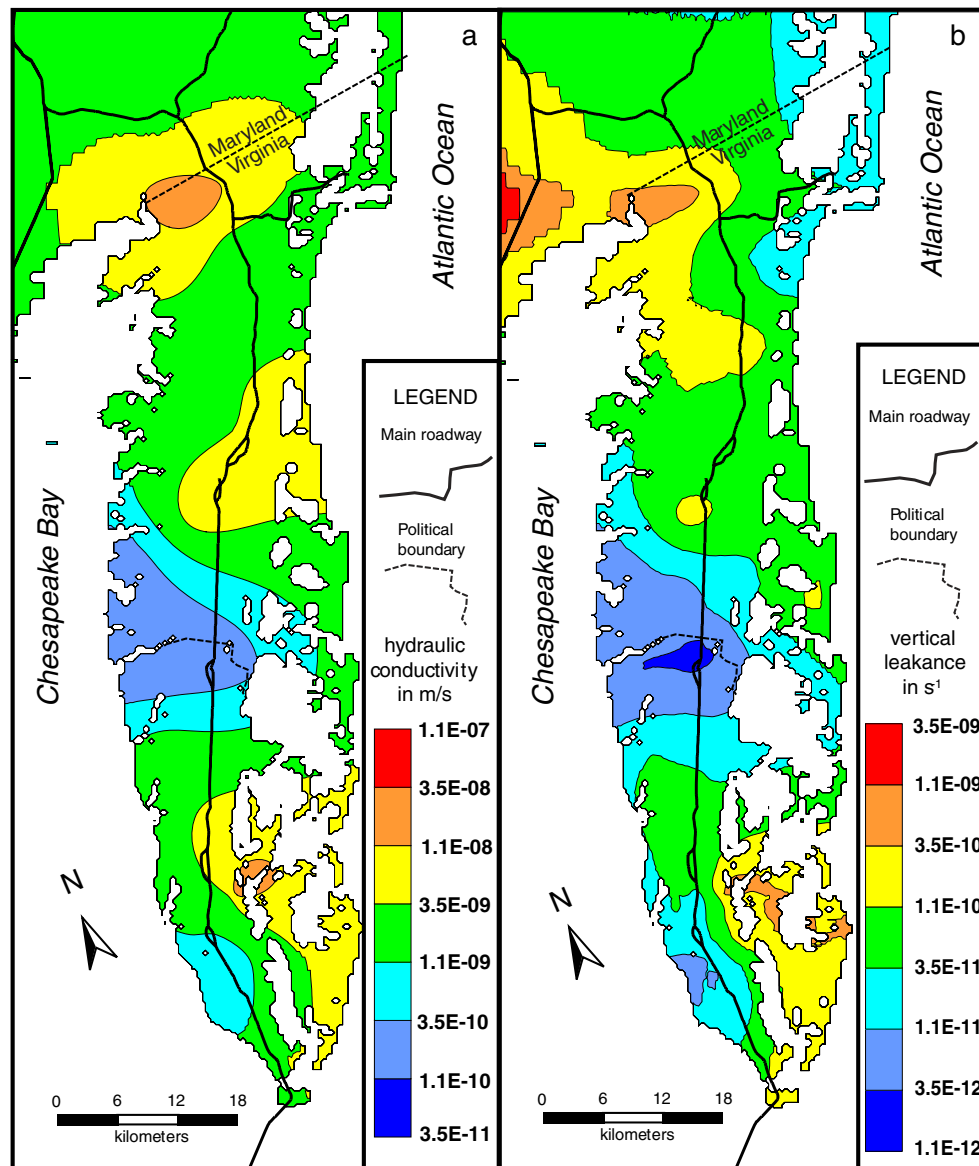


Fig. 9 The calibrated a hydraulic conductivity, and b vertical leakage of the upper Yorktown-Eastover confining unit

topography closely, and water levels decrease with increasing depth beneath the central ridge, reflecting a downward gradient and recharge. Water levels in the surficial aquifer exceed 6 m above mean sea level (amsl) along the ridge, whereas water levels in the lower aquifer usually do not exceed 3 m amsl.

Simulated water levels in the lower aquifer for 1980 and 2000 are shown in Fig. 11. Small cones of depression had developed in southern Northampton County by 1980, but water levels in that area recovered by 2000 because much of the withdrawal in that area had ceased. In central Accomack county, two simulated cones of depression persist through 2000 because of pumping associated with two large poultry-processing facilities. These simulated cones of depression are larger in 2000 than in 1980, and are of greatest lateral extent in the lower Yorktown-Eastover aquifer.

### Simulated chloride distribution

Chloride concentrations are used as a proxy for salinity in the model, where the chloride concentration of seawater was set at the mean ocean value of 19,000 mg/L. Establishing an initial chloride distribution for predevelopment conditions in the model was not a straightforward process. Often for such systems, an assumption is made that the system is at equilibrium with respect to current sea level and the current groundwater flow system. During the last ice age, the entire Chesapeake Bay and the Atlantic continental shelf were above sea level and received recharge of freshwater. The subsequent rise of sea level to present-day conditions was accompanied by the migration of the freshwater/seawater transition zone toward the present-day coastline. One can simulate a transition zone in an equilibrium position starting with fresh-water conditions everywhere beneath the present-day land surface and letting the simulation run for a time that

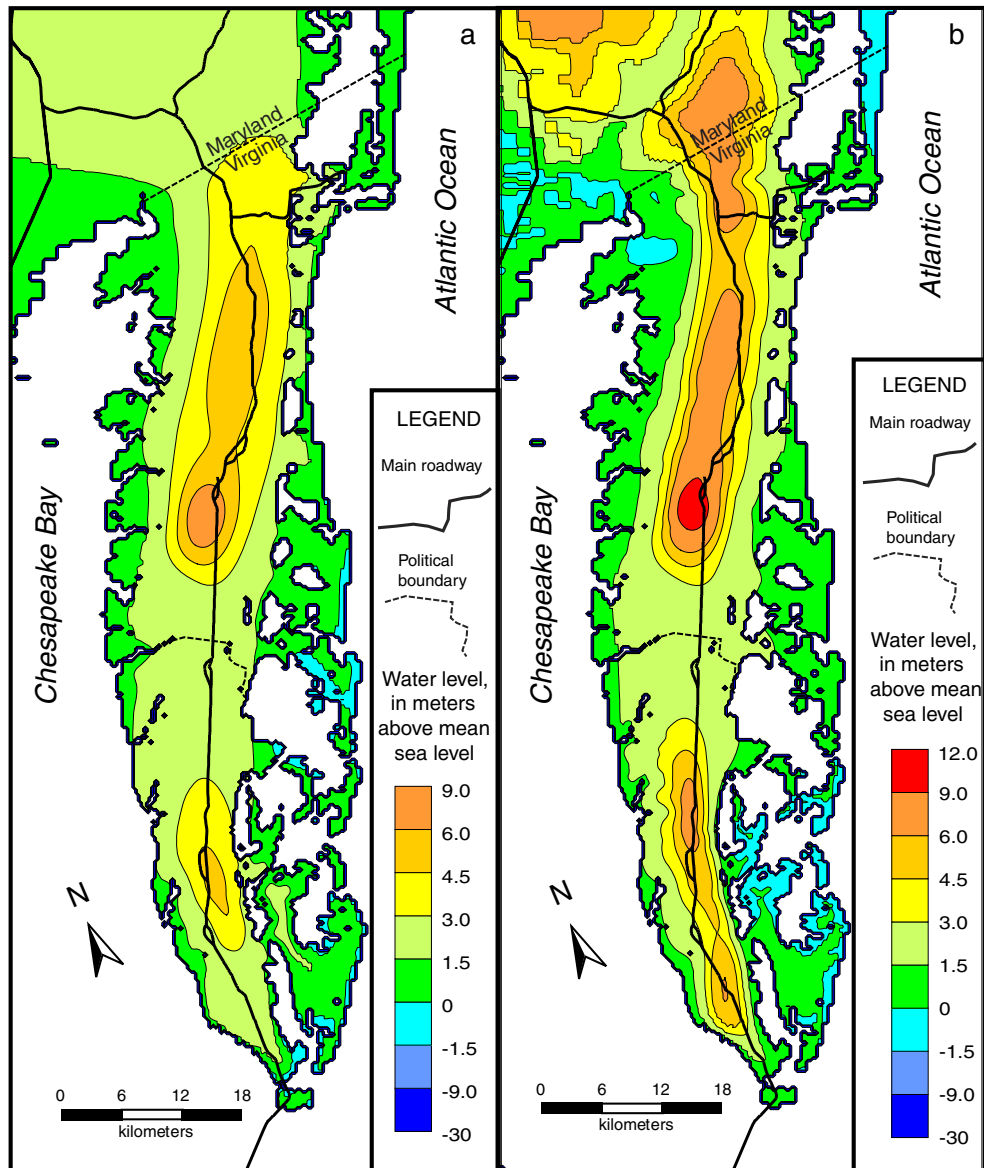


**Fig. 10** Simulated 1900 (predevelopment) water levels in the **a** lower and **b** upper Yorktown-Eastover aquifer

is long enough to reach equilibrium. This typically requires tens of thousands of years of simulation time. Such a simulation was run with the Eastern Shore model. A problem with this approach is that usually the resulting simulated equilibrium transition zone does not have chloride concentrations at the observation wells that match all or any of the observed chloride concentrations in the wells. Such was the case with the Eastern Shore model; some of the simulated chloride observations were too high, and others were too low. An alternative approach might be to attempt to create a three-dimensional transition zone in the model that matches the observations; the problem with this approach is that there are not enough observations to do this, and there is no easy way to make such a field reflect the flow conditions in the system without simulating the zone's position and distribution.

A different, but related, approach was taken in this study that attempted to make a realistic transition zone that also reflected the concentrations that were measured at the

observation wells. Little change was observed in chloride between the 1980's and 2003, and thus we used the 1980's values to represent pre-development values as the error associated with this approximation is much less than the certainty associated with the estimated position of the pre-development transition zone. An initial simulation was run starting with freshwater under all land cells and seawater under all water cells. This simulation was run to equilibrium, but snapshots of the chloride-concentration field were saved at various time steps. A comparison was then made between each observed chloride-concentration value above 100 mg/L and the simulated values. A time snapshot of the entire transition zone was assigned to each observation well according to the time at which the simulated chloride level best fit the chloride observation at that well. Some observation wells (especially on the bay side) never matched because observed chlorinity values exceeded all simulated values (the simulated transition

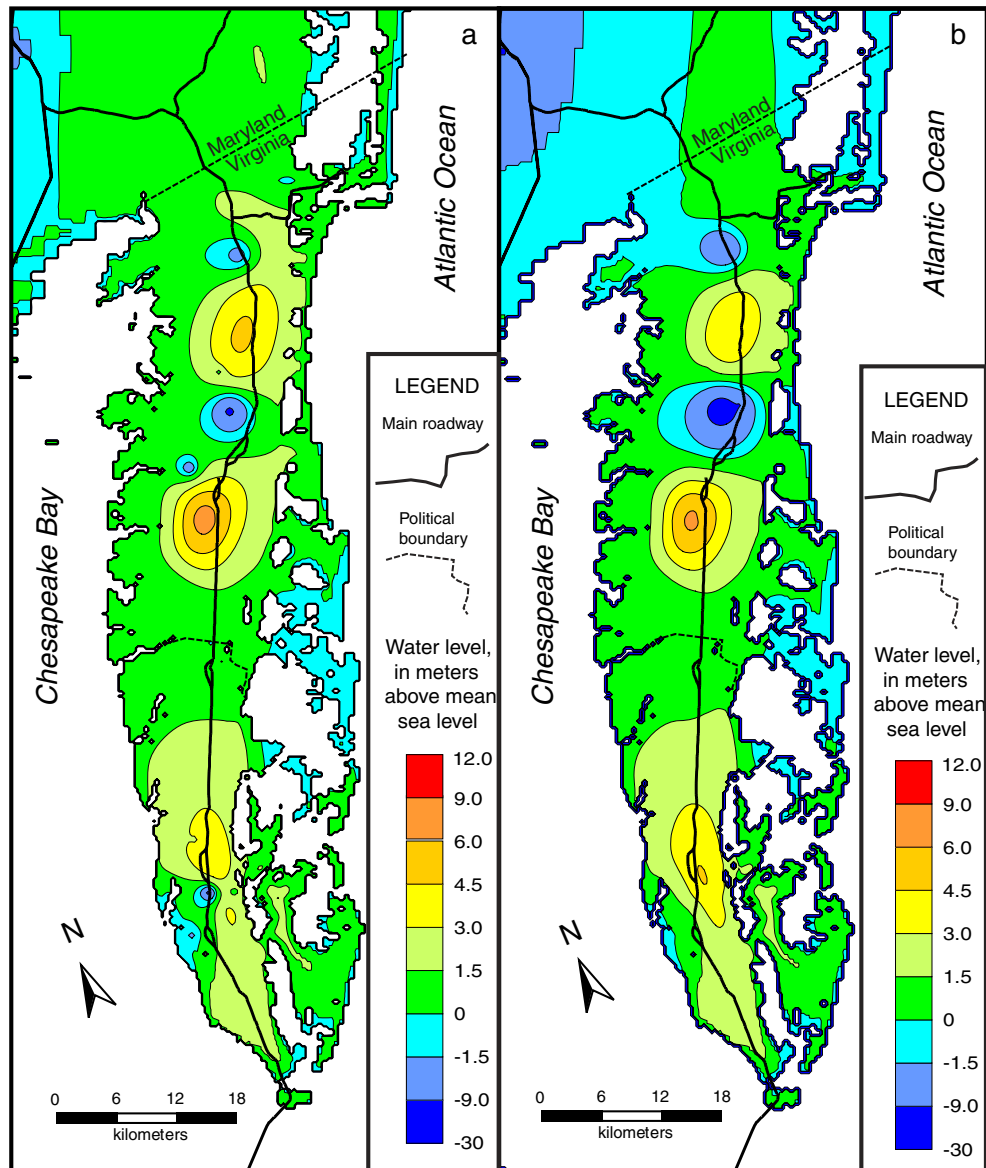


**Fig. 11** Simulated **a** 1980 and **b** 2000 water levels in the lower Yorktown-Eastover aquifer

zone never encroached far enough inland at equilibrium). For these wells, a snapshot of the entire transition zone was used that translated the equilibrium-simulated transition zone inland in a due easterly or westerly direction (along model rows) until a best match could be made to the observed chloride-concentration level. At this point in the process, each well had associated with it a snapshot of a chloride-concentration field for the entire model area that best fit the observed value at the well. These multiple fields were then combined into one smoothly varying field (that was still a best-fit at each observation well) by using the kriging routine that was used for the pilot points (Sanford et al. 2009a). In this context, the location of each observation well became the equivalent of the pilot point location.

Once the predevelopment chloride-concentration field was established, historical simulations were run to simulate the change in the chloride concentration that may have occurred because of pumping over the past century. Results

for the lower aquifer are shown in Fig. 12a. In general, it is difficult to see the difference in chloride by simply comparing the concentration fields themselves for 1900 and 2003. For this reason the changes in concentration between the two different years are shown in Fig. 12b. In the lower aquifer, increases in simulated chloride concentrations of greater than 100 mg/L can be observed around Cape Charles, east of Exmore, and near Chincoteague. Although the initial chloride condition is not at equilibrium with sea level, the regional response to this was very slow compared to saltwater intrusion that resulted from pumping.

The distribution of chloride, and thus seawater, beneath the Eastern Shore is three-dimensional, and vertical cross sections illustrate its distribution with depth (Fig. 13). Three cross sections are shown along rows 68, 180, and 288 of the model. The first section (Fig. 13a) is in the northern area near Chincoteague. The second section (Fig. 13b) is near Exmore, and the third section (Fig. 13c) is near Cape Charles. In areas

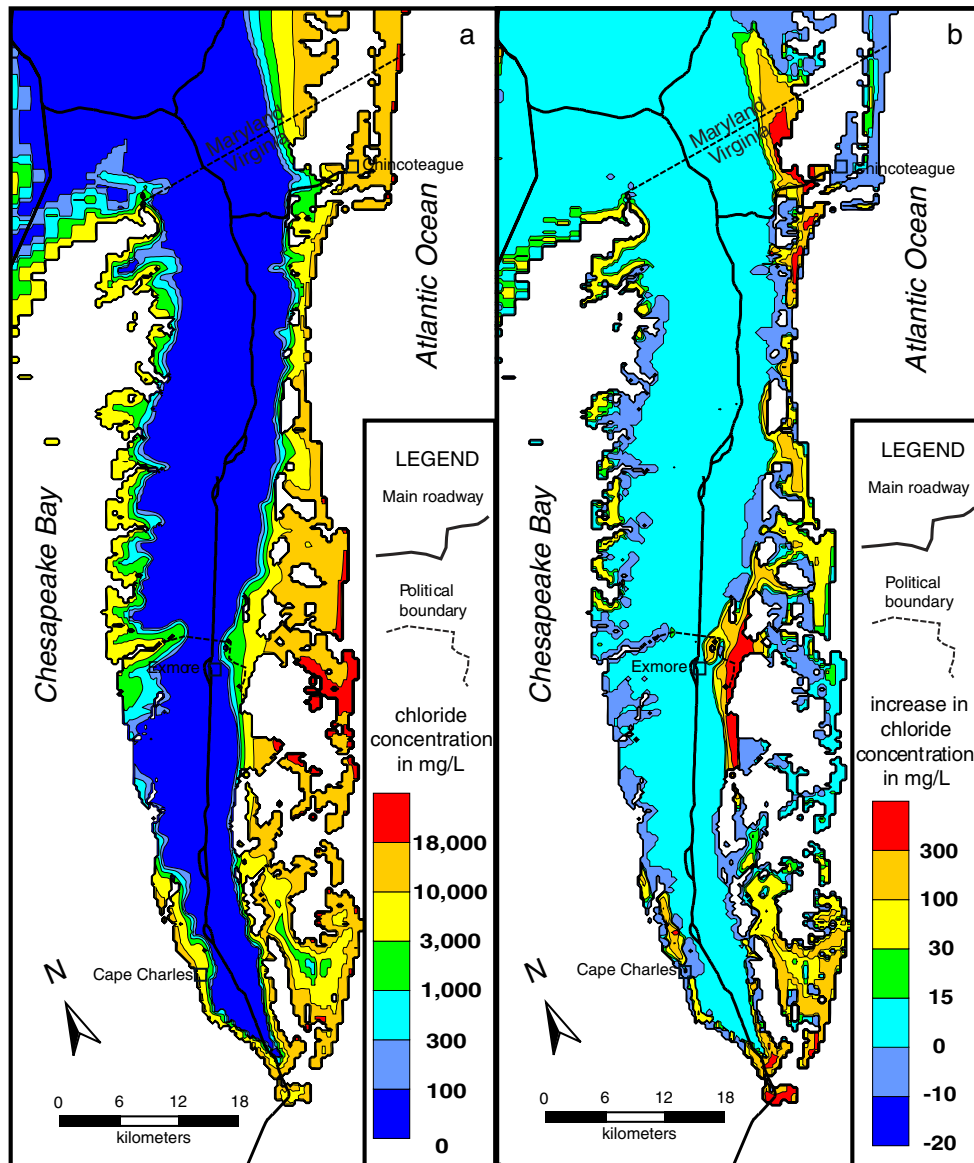


**Fig. 12** Maps showing simulated **a** chloride concentrations in 2003, and **b** changes in chloride concentrations between 1900 and 2003 in the lower Yorktown-Eastover aquifer

where the land surface is above sea level, chloride concentrations within the St. Marys confining unit were specified to increase slowly with depth in a manner similar to the salinity profile in a core take near Eastville (Sanford et al. 2009b). There is little other data from the Eastern Shore that indicate how salinity increases beneath the lower aquifer.

### Forecasting saltwater intrusion

The model developed in this study was intended to be used by state and local water managers to assess the impacts of future withdrawals on water conditions, including saltwater intrusion, on the Eastern Shore. In order to test the model in these types of future-scenario simulations, two different pumping rates were simulated until 2050: (1) pumping that continues at 2003 levels, and (2) pumping that is set at the total permitted withdrawal

rates for the Eastern Shore. The latter pumping rates are greater than the former.

The effect of pumping at the 2003 rates until 2050 is shown for the lower aquifer in Fig. 14a. The coastal region around Cape Charles has, between 2003 and 2050, simulated chloride increases of over 100 mg/L in 2050. The southernmost tip of the peninsula and Fisherman's Island have increases of over 300 mg/L. The region just east of Exmore and other areas near Chincoteague also have a simulated increase in chlorinity of over 300 mg/L.

Simulations until the year 2050 with total permitted withdrawal rates typically predict greater increases in chloride than those with 2003 withdrawal rates. Greater simulated increases in chloride are a result of higher simulated pumping rates. Patterns of chlorinity increases are somewhat similar to those from the 2003-pumping-rate scenario. The areas near Cape Charles, east of Exmore, and west of Chincoteague show very similar

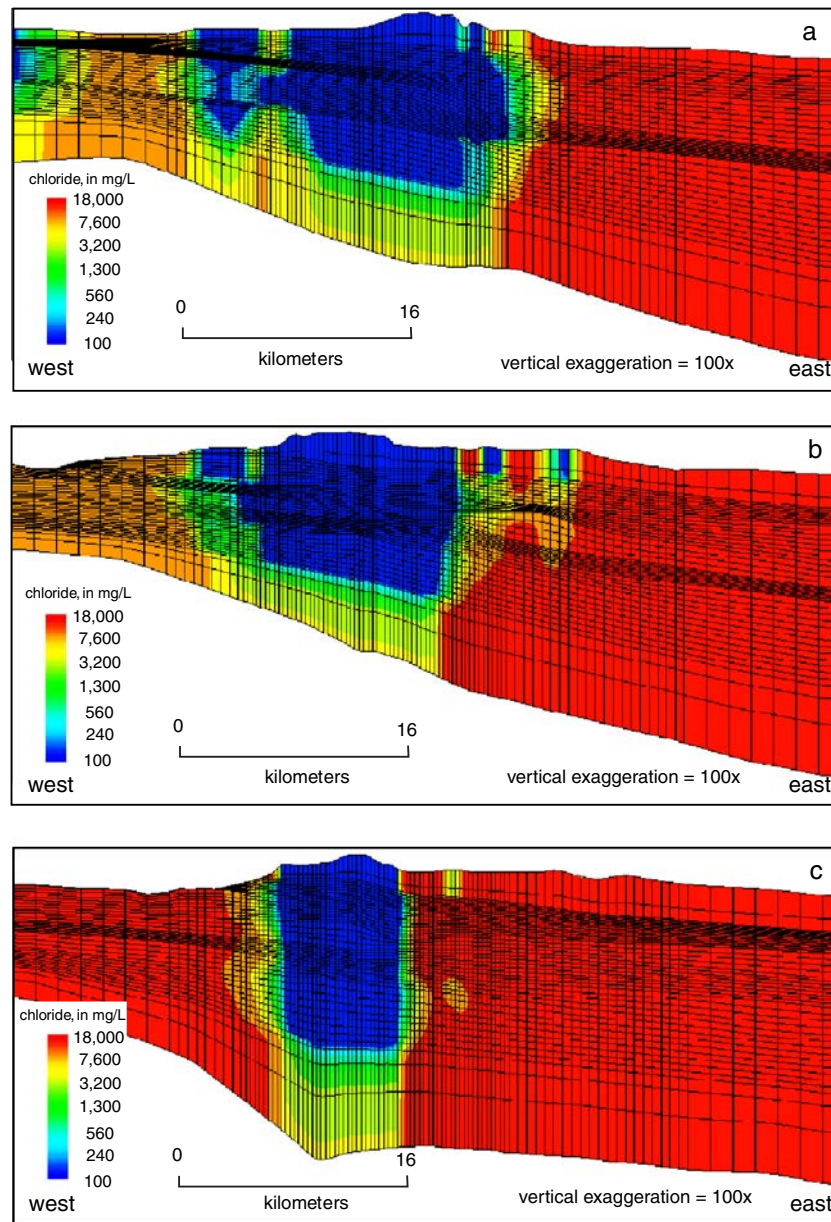


**Fig. 13** Cross-sectional views of simulated chloride concentrations in 2000 at model rows **a** 68, **b** 180, and **c** 288. See Fig. 4b for locations of model rows

chlorinity increase patterns to those of the 2003-rate scenario. Two additional areas of potential intrusion appear, however, in the lower aquifer (Fig. 14b). The simulated increase in chloride concentration near the eastern coastal area of central Accomack County is likely to be an effect from the two large cones-of-depression. Also, the entire southern end of the peninsula in Northampton County shows increases in simulated chlorinity of >100 mg/L.

Only a few of the observation wells show simulated chloride-concentration values that have a substantial rise between 1900 and 2050 (Fig. 15) under either 2003 or total-permitted withdrawal scenarios. These include wells near Chincoteague (SOW-115), south of Cape Charles (SOW-121), and east of Exmore (SOW-112). The well east of Exmore shows an additional increase in simulated

chloride concentration when the total-permitted-withdrawal scenario is simulated. The remaining wells did not show any additional increase in simulated chloride concentration.

## Discussion

This study demonstrates that it is feasible to simulate in three dimensions a freshwater lens that is 100 m deep in a peninsula that is 20 kilometers wide and over 100 km long. Accuracy in the transport equation had to be sacrificed, however, to maintain reasonable computation times. Forward flow simulations (density held constant) took approximately 2 h on a single PC and transport simulations took approximately 12 h. Automated parameter

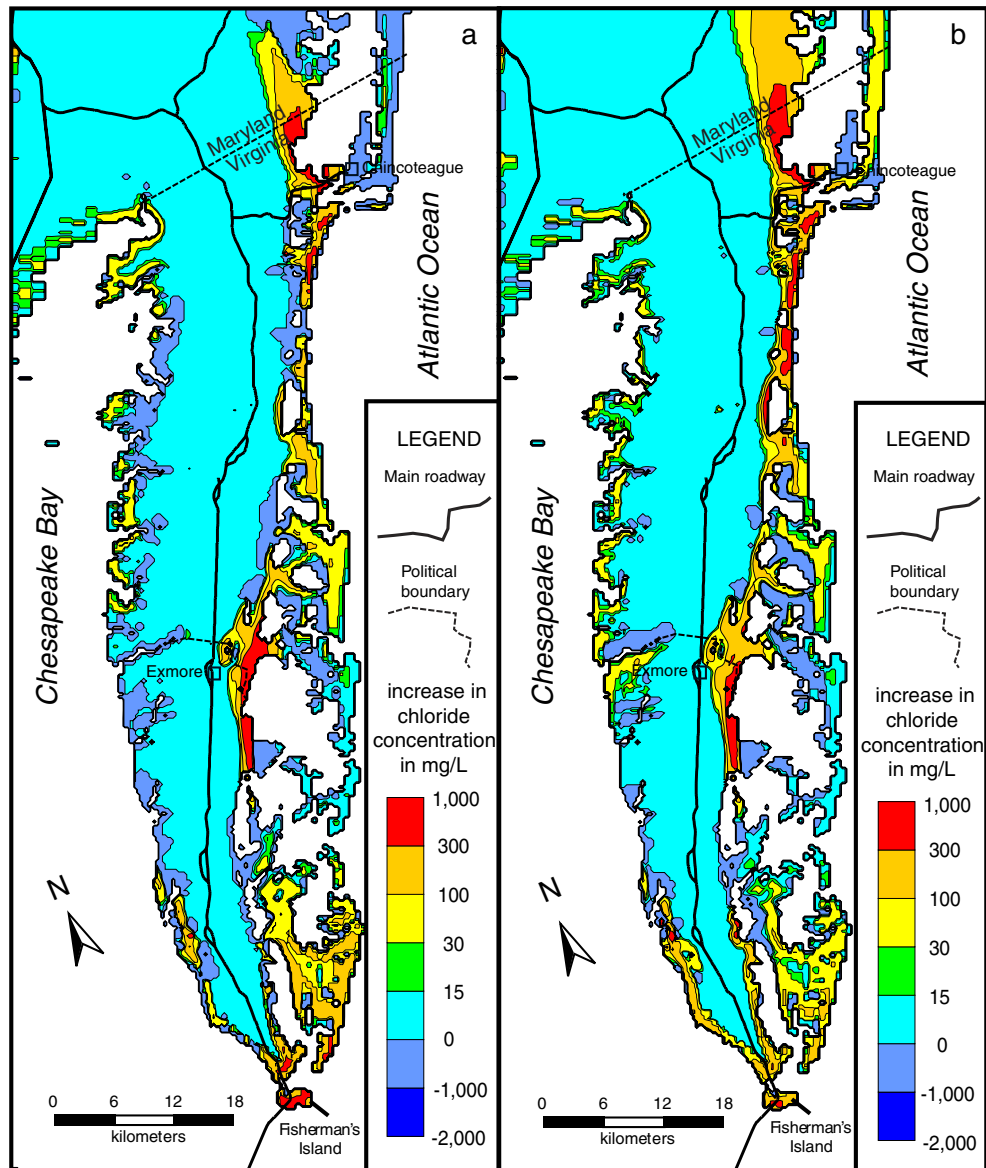


**Fig. 14** Changes in chloride concentrations in the lower Yorktown-Eastover aquifer from 2003 to 2050 assuming pumping after 2003 is for **a** 2003 pumping rates, and **b** total permitted withdrawal rates

estimation, which required hundreds of forward simulations, could only be performed with the flow simulations, and not simultaneously for all estimated parameters (Table 3). The model presented here contains substantial numerical dispersion. Upstream weighting was required to maintain numerical stability. Ideally, one would be able to quantify the amount of numerical dispersion in a model by rerunning the problem with a more finely discretized grid. Given that the limit of available computational speed and storage was already being reached, such a quantification was not an option. The lack of accuracy can be observed in a transition zone that is spread across several model layers vertically (Fig. 13), where individual cells range between 1 and 10 m thick. It has been demonstrated that natural transverse dispersivities in these zones are frequently less than 1 m and require vertical discretizations much less than 1 m to accurately simulate. The simulated transition zone has a

realistic appearance, but the numerical dispersion alone dictates that misfits to observed chloride values at wells should be expected, and in fact, occur. The model predicted negligible chloride concentration increases for most of the wells for which there were observed chloride concentrations (Table 2). Only a few wells had predicted chloride changes (SOW-112 and SOW-115, Fig. 15). The accuracy of those predictions is not expected to be high because of the numerical dispersion in the model. Thus the objective of creating a model that could forecast chloride increases at individual wells was not realized. Future simulation scenarios, or forecasts, may provide some general useful understanding of system behavior, but water-resource managers must be careful in trusting the accuracy of predictions at individual wells from a regional model.

Given the inability of the currently available computers to handle a simulation that is refined enough to accurately

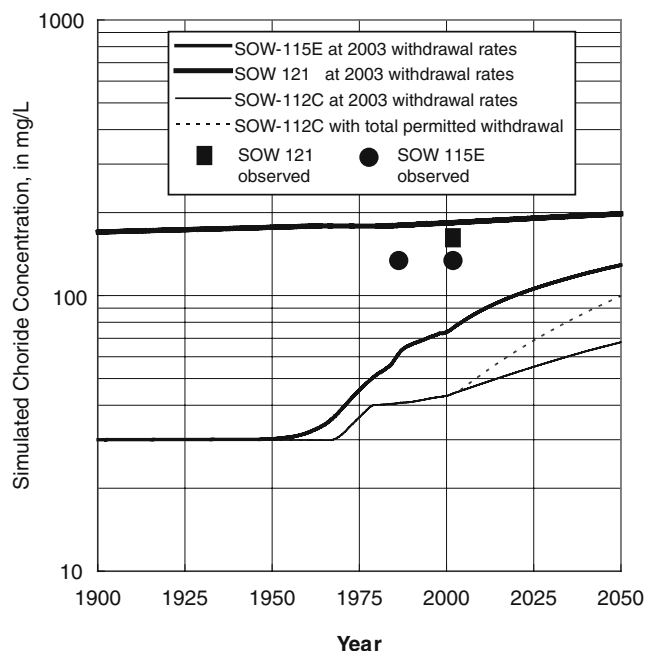


**Fig. 15** Simulated increases in chloride concentrations in certain wells. Observed chloride concentration for well 112C is off the scale at 1,550 mg/L. SOW is a well number prefix assigned by the Virginia State Water Control Board to all of the research well clusters at the time of well construction

simulate flow and transport equations as they apply to both a regional transition zone and to flow and transport in the vicinity of a well, an estimation was made of the computational power that would be required for a relatively accurate solution. Sufficient vertical discretization of a transition zone would require, say, 10-cm model layers. Horizontal discretization would need to be refined, perhaps, only in the vicinity of the wells of interest. So, spatially two or three orders of magnitude more cells would be required. A finer spatial discretization requires a finer time discretization for numerical stability. Time-step sizes would need to be approximately two orders of magnitude smaller in order to not require upstream weighting for numerical stability. Thus a computer with at least five orders of magnitude more computational speed (and storage) than used in this study would be needed to simulate the advective-dispersion equations accurately for the entire regional model. Given the current growth rate in computer speed and storage, such computer power is not likely to be seen any time in the near future. The only way to accurately simulate both a transition zone and the movement of saltwater near a well with available computer capabilities may be to refine the mesh only in the local area of interest.

The current computational challenge appears daunting, but it may not be ultimately the greatest challenge. Even if a computer were available with overwhelming or even infinite capability, that would not guarantee a simulation that could accurately forecast a salinity increase at a particular well. A groundwater model must not only solve the equations accurately, it must incorporate the field conditions accurately and with enough detail to be able to

mimic the actual flow and transport conditions in the field. Although hundreds of water-level and chemistry data were available for this study, they were insufficient to estimate hydraulic parameters in much spatial detail. Chloride concentrations were mostly measured in the fresher waters, and were not of sufficient number to create an initial concentration distribution of salinity within the three-dimensional framework of the peninsula. In the vicinity of the wells threatened by seawater intrusion, the data were also insufficient to increase the certainty of predictions there.

A number of different types of data are typically needed in much greater quantities to create a model that could give reasonably accurate predictions. The hydraulic conductivity field was estimated through automated inverse techniques, but high uncertainty was present for many regions in the model (Sanford et al. 2009a). Certainty was highest in areas where long-term withdrawals created pumping tests that were years to decades long. Such data existed in only a fraction of the model area. Porosity is constrained more than hydraulic conductivity, but values can vary locally on the meter to kilometer scale. Only values for total porosity were available. Effective porosity is necessary for relatively rapid movement at local scales such as transport in the vicinity of a well. The type of data most lacking that affected simulated concentrations were those that could define the initial concentration distribution in space. This system, like many coastal systems, does not appear to be in equilibrium with the last sea-level rise. Many such systems are far out of equilibrium (Meisler et al. 1985; Kooi and Groen 2001; Person et al. 2003, Hughes et al. 2009). For such systems, one must have an accurate initial concentration field to expect accurate simulated predictions. Yet typically very few data points are available in the more saline waters of a transition zone. Two approaches, neither of which may be acceptable options, are to assume equilibrium with sea level even when there is none, or to create an initial three-dimensional concentration field based only on the available data. In this study, a kriged initial concentration field was created in an attempt to best match the few observations yet create a distribution with a realistic position and shape. Also, without in situ concentration data near a site of interest, salinity predictions near that site cannot be made with any useful certainty. Thus, without abundant high-quality data in critical areas of interest, even an infinitely powerful computer cannot produce a simulation with accurate or even useful predictions for that area.

In spite of the challenges faced by the need for more data, there are some potential approaches that may prove to be partially productive in the near future. The first is the use of models that can be discretized both at the large and small scale. Finite element models (Voss and Provost 2002) can be used in such fashions if one can accommodate the greater effort required to build the input data sets for a variable-grid and variable-scale model. Graphical user interfaces are a necessity for such grid construction. Local-grid refinement is also becoming a more widely available option (Mehl and Hill 2002) for finite-difference models, where a finer “child” grid is constructed within a coarser regional “parent” grid

and solved simultaneously. To date these grid-refinement techniques have been used predominantly in groundwater flow or transport problems where transport may only be required in the child grid. Local-grid refinement for saltwater intrusion would by nature include transport at both scales. Inclusion of local-grid refinement is currently under development for SEAWAT (C. Langevin, personal communication, 2009 U. S. Geological Survey). Another potential approach that was not used in this study was the inclusion of geophysical data (Stewart 1999). Airborne resistivity can help to interpolate between sparse data points (e.g., Fitterman and Deszcz-Pan 1998). Subsurface resistivity can help map out the transition zone deeper under ground. Such a resistivity survey has been reported for the Eastern Shore of Virginia (Nowroozi et al. 1999), but was not used in this study because the combination of salinity variations and variable clay content created uncertainty in the estimated salinity distributions. In spite of the current challenges in simulating saltwater intrusion, and the potential use of certain methods to combat these challenges, it is prudent at present to maintain realistic expectations of the certainty of model predictions given the typical paucity of data. Forecasting changes in chloride levels at specific wells is still accompanied by a high level of uncertainty compared to that of forecasting the long-term movements of a transition zone.

**Acknowledgements** This study was funded in part by the United States Geological Survey Office of Groundwater, the Virginia Department of Environmental Quality, and the Accomack-Northampton Planning District Commission.

## References

- Bear J, Cheng AH-D, Sorek S, Ouazar D, Herrera I (1999) Seawater intrusion in coastal aquifers: concepts, methods and practices. Theory and Applications of Transport in Porous Media 14. Kluwer, Dordrecht, The Netherlands
- Cooper HH Jr, Kohout FA, Henry HR, Glover RE (1964) Sea water in coastal aquifers. US Geol Surv Water Supply Pap 1613-C
- Cox RA, Nishikawa T (2001) A new total variation diminishing scheme for the solution of advective-dominant solute transport. Water Resour Res 27:2645–2654
- Cushing EM, Kantrowitz IH, Taylor KR (1973) Water resources of the Delmarva Peninsula. US Geol Surv Prof Pap 822
- Doherty J (2002) Manual for PEST, 5th edn. Watermark, Brisbane, Australia
- Domenico PA, Mifflin MD (1965) Water from low permeability sediments and land subsidence. Water Resour Res 4:563–576
- Fennema RJ, Newton, VP (1982) Ground water resources of the Eastern Shore of Virginia. Commonwealth of Virginia State Water Control Board Planning Bulletin 332, Commonwealth of Virginia State Water Control Board, Richmond, VA
- Fitterman DV, Deszcz-Pan H (1998) Helicopter Em mapping of saltwater intrusion in Everglades National Park, Florida. Explor Geophys 29:240–243
- Guo W, Langevin CD (2002) User's guide to SEAWAT: a computer program for simulation of three-dimensional variable-density ground-water flow. US Geol Surv Open-File Rep 01-434
- Halford KJ, Hanson RT (2002) User guide for the drawdown-limited, multi-node well (MNV) package for the US Geol Surv modular three-dimensional finite-difference ground-water flow model, versions MODFLOW-96 and MODFLOW-2000. US Geol Surv Open-File Rep 02-293
- Heywood CE, Pope JP (2009) Simulation of groundwater flow in the Coastal Plain aquifer system of Virginia. US Geol Surv Sci Invest Rep 2009-5039
- Hughes JD, Vacher HL, Sanford WE (2009) Temporal response of hydraulic head, temperature, and chloride concentrations to sea-level changes, Floridan aquifer system, USA. Hydrogeol J 17:793–816
- Kooi H, Groen J (2001) Offshore continuation of coastal ground-water systems: predictions using sharp-interface approximations and variable-density flow modeling. J Hydrol 246:19–35
- Langevin CD, Shoemaker WB, Guo W (2003) MODFLOW-2000, the U.S. Geological Survey modular ground-water model: documentation of the SEAWAT-2000 version with variable-density flow process (VDF) and the integrated MT3DMS transport process (IMT). US Geol Surv Open-File Rep 03-426
- McFarland ER, Bruce TS (2006) The Virginia Coastal Plain hydrogeologic framework. US Geol Surv Prof Pap 1731
- Mehl S, Hill MC (2002) Development and evaluation of a local grid refinement method for block-centered finite-difference ground-water models using shared nodes. Adv Water Resour 25:497–511
- Meisler H, Leahy PP, Knobel LL (1985) Effect of eustatic sea-level changes on saltwater-freshwater relations in the northern Atlantic Coastal Plain. US Geol Surv Water Supply Pap 2255
- Meng AA III, Harsh JF (1988) Hydrogeologic framework of the Virginia Coastal Plain. US Geol Surv Prof Pap 1404-C
- Mixon RB (1985) Stratigraphic and geomorphic framework of uppermost Cenozoic deposits in the southern Delmarva Peninsula, Virginia and Maryland. US Geol Surv Prof Pap 1067-G
- Neretnieks I (1981) Age dating of groundwater in fissured rocks: influence of water volumes in micropores. Water Resour Res 17:421–422
- Nowroozi AA, Horrocks SB, Henderson P (1999) Saltwater intrusion into the freshwater aquifer in the eastern shore of Virginia: a reconnaissance electrical resistivity survey. J Appl Geophys 42:1–22
- Person M, Dugan B, Swenson JB, Urbano L, Stott C, Taylor H, Willett M (2003) Pleistocene hydrogeology of the Atlantic continental shelf, New England. Geol Soc Am Bull 115:1324–1343
- Pinder GF, Cooper HH Jr (1970) A numerical technique for calculating the transient position of the saltwater front. Water Resour Res 9:1657–1669
- Poeter EP, Hill MC (1998) Documentation of UCODE, a computer code for universal inverse modeling. US Geol Surv Water Resour Invest Rep 98-4080
- Pope JP, McFarland ER, Banks RB (2007) Private domestic well characteristics and the distribution of domestic withdrawals among aquifers on the Virginia Coastal Plain. US Geol Surv Sci Invest Rep 2007-5250
- Post VEA (2005) Fresh and saline groundwater interaction in coastal aquifers: is our technology ready for the problems ahead? Hydrogeol J 13:120–123
- Richardson DL (1994) Hydrogeology and analysis of the ground-water-flow system of the Eastern Shore, Virginia. US Geol Surv Water Suppl Pap 2401
- Robbins EI, Perry WJ Jr, Doyle JA (1975) Palynological and stratigraphic investigations of four deep wells in the Salisbury Embayment of the Atlantic Coastal Plain. US Geol Surv Open-File Rep 75-307
- Sanford WE, Konikow LF (1985) A two-constituent solute-transport model for ground water having variable density. US Geol Surv Water Resour Invest Rep 85-4279
- Sanford WE, Pope JP, Nelms DL (2009a) Simulation of ground-water-level and salinity changes in the Eastern Shore, Virginia. US Geol Surv Sci Invest Rep 2009-5066
- Sanford WE, Voytek MA, Powars DS, et al (2009b) Pore-water chemistry from the ICDP-USGS corehole in the Chesapeake Bay impact structure: implications for paleohydrology, microbial habitat, and water resources. In: Gohn GS, Koeberl C, Miller KG, Reimold WU (eds) Deep Drilling Project in the

- Chesapeake Bay impact structure. *Geol Soc Am Spec Pap* 458, p. 869–892, doi:10.1130/2009.2458(36)
- Segol G, Pinder GF (1976) Transient simulation of saltwater intrusion in southeastern Florida. *Water Resour Res* 12:65–70
- Sinnott A, Tibbotts GC Jr (1968) Ground-water resources of Accomack and Northampton Counties, Virginia. *Min Resour Rep* 9, Virginia Division of Mineral Resources, Richmond, VA
- Speiran GK (1996) Geohydrology and geochemistry near coastal ground-water-discharge areas of the Eastern Shore, Virginia. *US Geol Surv Water Supply Pap* 2479
- Stewart MT (1999) Geophysical investigations. In: Bear J, Cheng AHD, Sorek S, Ouazar D, Herrera I (eds) *Seawater intrusion in coastal aquifers: concepts, methods and practices*. Kluwer, Dordrecht, The Netherlands
- Todd DK (1959) *Ground water hydrology*. Wiley, New York
- Voss CI (1984) SUTRA Saturated-Unsaturated TRANsport: a finite-element simulation model for saturated-unsaturated fluid-density-dependent ground-water flow with energy transport or chemically-reactive single-species solute transport. *US Geol Surv Water Resour Invest Rep* 84-4329
- Voss CI, Provost AM (2002) SUTRA: a model for saturated-unsaturated variable-density ground-water flow with solute or energy transport. *US Geol Surv Water Resour Invest Rep* 02-4231
- Voss CI, Souza WR (1987) Variable density flow and transport simulation of regional aquifers containing a narrow freshwater-saltwater transition zone. *Water Resour Res* 23:1851–1866
- Zheng C, Bennett GD (1995) *Applied contaminant transport modeling: theory and practice*. Wiley, New York